Using the Error Propagation Approach and Effective Distance Relating to Reference Evapotranspiration Considering Alternative Data

A dissertation submitted in partial fulfillment of the requirements

The degree of Doctor of Philosophy (Ph.D.)

Laboratory of Water Resources Engineering

Department of Environmental Science and Technology

Graduate School of Bioresources, Mie University

Homayoon Ganji

March, 2019

The undersigned have examined the dissertation entitled "**Using the Error Propagation Approach and Effective Distance Relating to Reference Evapotranspiration Considering Alternative Data**" presented by Homayoon Ganji, a candidate for the degree of Ph.D. and hereby certify that it is worthy of acceptance.

Date

Prof. Takamitsu Kajisa
Supervisor

Date

Prof. Hajime Narioka
Committee member

Date

Prof. Ken Oono
Committee member

Date

Assoc. Prof. Kenji Okajima
Committee member

Acknowledgments

It is not an easy task to acknowledge everybody who contributed to this thesis, but let's first to recognize the strong encouragement from my kind family and my lovely wife Ms. Nahide Faiaz, to follow my way. The work presented in this thesis was possible because of the strong contribution of my supervisors whom I would like to acknowledge very much.

My special attention goes to Prof. Takamitsu Kajisa for working with me together on all the ideas of this thesis and the related papers.

I would like to extend my appreciation to Prof. Hajime Narioka, Prof. Ken Oono and Associate professor Kenji Okajima, for their efficient comments, supports and encouragement mainly on my future courier.

Warm thanks are extended to my best friends Mr. Abdul Saboor Rahmany and Dr. Behroze Rostami for their close contact and contribution.

Finally, I wish to acknowledge the JICA Peace Project, Kubota foundation and JASSO, for the fund provided. Last but not least, thanks to the Ministry of Higher Education of the Islamic Republic of Afghanistan, particularly Badghis Agricultural Faculty for the opportunity given.

Homayoon Ganji

Abstract

Reference evapotranspiration (ET_0) is the main component of the irrigation water depth, which can be either measured directly or calculated using theoretical models. However, to achieve high efficiency in irrigation water depth in a semi-arid environment, information is limited on reliable estimates of ET_0.

Many different models have been developed for calculating ET_0 based on their daily performances under the given climatic conditions in the world. The United Nations Food and Agriculture Organization (FAO) proposed a model for estimating the standard ET_0, known as the Penman-Monteith model (FAO-56PM). The accuracy of the FAO-56PM model is sufficiently high to be recommended as the sole method for calculating ET_0 in the cases where the necessary data are available.

In this study, the FAO-56PM model was selected as the base model for examining in location where is exposed to relatively strong windy semi-arid conditions i.e. Afghanistan, especially with alternative data. The second part of this study focuses on the error estimation using error propagation approach. Furthermore, the effective distance for sharing the climatic data relating to ET_0 was proposed in the cases when some data are missing.

The results from the analysis confirmed that, the FAO-56PM model was the best model among the six well-known models in the investigated semi-arid areas in Afghanistan, however, its accuracy decreased in the high rates (>10 mm d^{-1}). A serious limitation to this models is high meteorological data demand, thereby limiting its utility in data-sparse areas. Some alternative procedures have been proposed by FAO to overcome with missing data challenges, however, the alternative procedures to compensate the missing data of relative humidity and wind speed were found erroneous in those semi-arid places that were exposed to a strong wind speed condition. To overcome this problem, this study suggested an

effective distance which is the upper limit of distance for data sharing between the stations. This is the distance within that range sharing data leads smaller error than that of using the FAO's alternative procedures for obtaining the alternative data. From the approximated semivariograms model's equation and the error theory, the effective distance could be established along the investigated distance at which the standard error was smaller than the alternative error resulted from the alternative data. This was the case corresponding to the data of solar radiation and actual vapor pressure. There was no effective distance established in the case of wind data.

To confirm the validity of ET_0 when calculated with alternative data in a certain area, root mean square error ($RMSE$) is needed to be calculated. However, $RMSE$ does not explain the source of error in a model equation. In this study, the error propagation approach was used to estimate $RMSE$ and to quantify the source of error. It was found that the error in the ET_0 estimation is not only related to the alternative data, while related to the combination of the variables in a model equation as well. This property is very useful when improving meteorological data obtained using alternative proposals or when improving the FAO-56PM formula. These two improvements correspond to the two components that constitute the theoretical expression of error propagation.

Table of Contents

List of Tables

List of Figures

Chapter One

Introduction and Methodology

1.1. Introduction

ET is defined as a physical processes whereby liquid water vaporized into the atmosphere from evaporating surfaces (Penman, 1948; Li and Lyons, 1999; Allen et al., 1998). Indeed, water is lost by evaporation on the one hand from the soil surface, lakes, rivers etc., and on the other hand from crop by transpiration. The two processes occur simultaneously as the combination of the two functions is referred to as ET (Allen et al., 1998; Su, 2002; Kalma et al., 2008).

ET is presented in different concepts as the two commonly used concepts are potential evapotranspiration (ET_p) and reference evapotranspiration (ET_0). In the late 1940s and 50s the ET_p concept was first introduced by Penman and it is defined as "the amount of water transpired in a given time by a short green crop, completely shading the ground, of uniform height and with adequate water status in the soil profile." In this definition, the ET rate is not related to a specific crop. Therefore, the main confusion with the ET_p definition is that there are many types of horticultural and agronomic crops that fit into the description of short green crop (Irmak and Dorota, 2003). To avoid ambiguities, the concept of ET_0 introduced by irrigation engineers and researchers in the late 1970s and early 80s. The ET_0 process is occurred from a reference surface, not short. The reference surface is a hypothetical grass reference crop with an assumed crop height of 0.12 m, a fixed surface resistance of 70 s m^{-1} and an albedo of 0.23 (Batchelor, 1984; Morton, 1990; Hanson, 1991). The concept of the ET_0 is used to introduce the evaporative demand of the atmosphere apart from the crop type, crop development and management practice. As water abundantly is available at the reference evaporating surface, soil factors don't affect ET_0. Relating ET_0 to an especial reference provides a reference to which ET_0 from other surfaces can be related. Therefore, it is not needed to define a separate ET level for each crop and stage of growth.

The two parameters of hydrology, evaporation from open water and ET from vegetated surfaces, are critical parameters. Justified efforts are made to measure and estimate these parameters. To measure these two parameters a range of techniques, form the evaporation pan to remote sensing techniques, have been progressed (Abtew and Assefa, 2013). The pan evaporation method, lysimeters (weighing lysimeter and water balance lysimeter), the eddy correlation method, Bowen ration method, and satellite-based methods are the methods that have been using to measure the evaporation and ET.

The common approach for most applicants is the estimation methods. Evaluation of methods with respect to the accuracy needed, available input data, and cost of data generation are the primary requirements to select a method for a specific application (Abtew and Assefa, 2013). A multitude of methods have been reported in the literature for estimating ET_0 (Pereira and Pruitt, 2004; Alexandris et al., 2005). The empirical models are widely used even some of them are most complex considering the input data. The empirical models have mainly been based on the climatological data, because of the difficulty of making direct measurements of ET_0. In general, three groups of methods (simple methods, complex methods and remote sensing methods) are listed in the literatures that are being used to estimate ET_0 worldwide. These three groups can be fitted in one of the following four methods which are vary based on their requirements. The pan method, temperature-based methods, radiation-based methods, and mass transfer methods (Abtew and Melesse, 2013). Most of the equations were developed for use in specific studies and are most appropriate for use in climates similar to where they were developed. It is not uncommon to use an equation for determination of evaporation from open water that was actually developed for determination of potential evapotranspiration from vegetated lands, and vice versa (Winter and Rosenberry, 1995).

The high rate of ET_0 robust its importance in agricultural regions, especially in the areas facing water scarcity. The agricultural sectors pay more attentions to the optimal estimation of ET_0, which is extremely important in the field of irrigation water saving and cost saving as well. The optimal estimation of ET_0 is possible through the application of those methods/models which offering high accuracy and efficiency with lower costs and less data demand when estimating ET_0. Although, some models i.e. FAO-56PM method, has been recommended as the standard method that offering high accuracy, however, this model has its own limitations i.e. high data demand, which are often not being recording in most of the stations, especially in developing countries. This property limiting the application of this model in such areas. There are some alternative models which require less data, recommended in the cases if the FAO-56PM model is difficult to be used. As well as, some alternative procedures are recommended in the literatures (i.e. FAO paper No. 56) for estimating the necessary data when the actual records are missing. Therefore, assessing some of the well-known models those are easier to be applied, and the alternative procedures for estimating the missing data, is needed in a given region to ensure the estimation of ET_0 with high accuracy and efficiency. At the beginning, from the calculation of the irrigation water volume we realized that ET_0 is extremely high (above 10 mm d^{-1}) in the strong windy semi-arid area (i.e. the West region of Afghanistan). This size is big enough to be seen in the most of the places worldwide and has a lot of unexpectedness.

Considering the high rate of ET_0 in areas facing water scarcity in one side, and data scarcity for estimating ET_0 in the other side, it is essential to examine ET_0 with the aim to provide clear information about the factors affecting the accuracy of ET_0 when calculating the irrigation water volume for agricultural purposes. In order to contribute in managing irrigation water volume, we examined the ET_0 estimation with different models and, as well as, with alternative data, with the aim of confirm a model and proposing a better way for estimating ET_0 with possible high accuracy in areas facing data scarcity. To achieve the aim, few studies were conducted with the following overall objectives:

1) To examine ET_0 with different models as well as with alternative data those estimated using the FAO's recommendations.
2) To examine the FAO-56PM model using error propagation approach.
3) To suggest a methodology for obtaining the missing data relating to the ET_0 estimation.

1.2. Methodology

In this thesis, the FAO-56PM model was used as the base model for estimating ET_0. The FAO-56PM model which becomes the well-known "Penman-Monteith" equation, developed when some crop resistance terms introduced in the original Penman equation by (Monteith, 1965). This equation is a physically based approach which can be used without local calibration. This property demonstrated its robustness (Temesgen et al., 2005). The FAO-56PM equation is lack of wind function instate it has aerodynamic and surface resistance terms, this equation is known as the Penman-Monteith (1965) equation. Later, in May 1990, FAO organized a consultation of experts and researchers in collaboration with the International Commission for Irrigation and Drainage and with the World Meteorological Organization, to review the FAO methodologies on crop water requirements and to advice on the revision and update of procedures. The panel of experts recommended the adoption of the FAO-56PM combination method as a new standard for ET_0 and advised on procedures for calculating the various parameters. Allen et al. (1998) developed guidelines for computing crop water requirements, in the FAO paper No.56, this is given as **Eq. 1**.

The FAO-56PM method was developed by defining the reference crop as "a hypothetical crop with an assumed height of 0.12 m, with a surface resistance of 70 s m^{-1} and an albedo of 0.23, closely resembling the evaporation from an extensive surface of green grass of uniform height, actively growing and adequately watered."

$$ET_0 = \frac{0.408\Delta(R_n - G) + \gamma \frac{900}{T_{Ave} + 273} u_2 (e_s - e_a)}{\Delta + \gamma(1 + 0.34u_2)} \quad (1)$$

$$R_n = (1 - 0.23)R_s - \sigma \frac{T_{max} + T_{min}}{2} \left(0.34 - 0.14\sqrt{e_a}\right) \left(1.35 \frac{R_s}{R_{so}} - 0.35\right) \quad (2)$$

$$R_s = \left(0.23 + 0.50 \frac{n}{N}\right) R_a \quad (3)$$

$$e_a = \frac{RH_{mean}}{100} e_s \quad (4)$$

$$e_s = \frac{0.6108 exp\left[\frac{17.27 T_{min}}{T_{min} + 237.3}\right] + 0.6108 exp\left[\frac{17.27 T_{max}}{T_{max} + 237.3}\right]}{2} \quad (5)$$

where, ET_0 is the reference evapotranspiration (mm d^{-1}), Δ is the slope of the vapor pressure curve (kPa), R_n is the net radiation estimated with solar radiation (MJ m^{-2} d^{-1}), G is the soil heat flux density (MJ m^{-2} d^{-1}), γ is the psychrometric constant (kPa $°C^{-1}$), T_{Ave} is the daily average air temperature (°C), u_2 is the daily average wind speed (m s^{-1}), e_s is the saturation vapor pressure (kPa), e_a is the actual vapor pressure (kPa), R_s is the solar radiation (MJ m^{-2} d^{-1}), α is the albedo (0.23), σ is the Stefan-Boltzmann constant, R_{so} is the clear-sky solar radiation (MJ m^{-2} d^{-1}), RH_{mean} is the mean relative humidity (%).

The parameters that include in the above equations (**Eq. 1-5**) can be obtained via the methods explained in the Appendix 1.

Chapter Two

Re-Examining the Validity of Reference Evapotranspiration Estimation in Herat, Afghanistan

2.1. Background

The aim of this study is to identify the adaptable model for estimating ET_0 when calculating irrigation water depth, in Herat province. Many different models have been developed for calculating the ET_0 based on their daily performances under the given climatic conditions in the world. In this chapter, six well-known models, the Penman-Monteith (ET_{0PM}), Hargreaves (ET_{0Hrg}), Hamon (ET_{0Ham}), Thornthwaite (ET_{0Trw}), Solar radiation based (ET_{0Rs}) and Net radiation based (ET_{0Rn}), and the pan evapotranspiration (ET_{pan}) models were selected to estimateET_0 based on their daily performance under the climatic condition of Herat.

The accuracy of the FAO-56PM model is sufficiently high to be recommended as the sole method for calculating ET_0 in the cases where the necessary data are available (Allen et al., 1998). However, the only limitation to the Penman family of models is that they require many meteorological dataset, thereby limiting their utility in data-sparse areas (Hanson 1998).

In the West region of Afghanistan, most organizations working in the field of agriculture and water supply, estimate the ET_0 rate using the software developed by FAO (CROPWAT). However, there is still no any research has been conducted to contrast different well-known methods to find whether any other model is adaptable for estimating ET_0 in the West region or not. Because the application of CROPWAT is not easy for everyone due to its complexity.

Based on the requirements, in this study we compared the ET_0 estimation using three temperature-based methods (ET_{0Trw}, ET_{0Hrg} and ET_{0Ham}), two radiation-based methods (ET_{0Rs} and ET_{0Rn}), and one aerodynamic plus energy budget approach (ET_{0PM}).

The temperature-based methods are simple models and are easy applied in those areas where the required input data are available, whereas the aerodynamic plus energy budget approach is a complex model which requires various input dataset. Therefore, its application is not easy in the areas where the input dataset is limited. Based on the different requirements of the models, six well-known models were selected for comparison with ET_{pan} to identify the suitable model for estimating ET_0 when calculating irrigation water volume, in Herat province.

2.2. Data and Analyzing Method

Herat Province in the West region of Afghanistan was selected as the study area. Herat is characterized by strong winds during the summer and arid to semi-arid climate conditions. The data were observed in the "Urdu Khan" regional agricultural research station which is located at a latitude of 34° 31' N and a longitude of 62° 22' E with an elevation of 964 meters. It lies in "Urdu Khan" village, 5.8 kilometers southeast of Herat city, shown in **Figure 2-1**. A strong wind known as the "120-day winds" persists from early June until late September with a strong average force of 7.01 m s^{-1} (Ganji et al., 2014). Based on the data observation in 2009, the maximum mean annual air temperature was around 37.5°C, and the minimum air temperature was 0.5°C. The total precipitation was recorded as 345.6 mm $year^{-1}$, and the daily average relative humidity was 41.3%.

As very little of the pan evaporation (E_{pan}) data was available, the data from 2009 was only used in the calculation. Variety of sources listed in **Table 2-1** were used for data collection.

2.2.1. Models Description

In this study, six different well-known models were selected for the ET_0 estimation. Based on the data requirements the selected models including the aerodynamic plus energy budget model, three temperature-based models, and two radiation-based models.

The FAO-56PM (**Eq. 1**) was one of the applied models. As stated emailer, this model is known as the aerodynamic energy budget model which requires different kinds of data for calculation. This models is not so easy to be used in the data scarce areas (**Eq. 1**).

The temperature-based modes are simpler models and are easily applied in areas where the required input data are available. Temperature-based models require fewer data, mainly air temperature data, for calculation. There are several models air temperature based models of which three different well-known models were selected in this study.

One of the temperature-based model is Thornthwaite model. Thornthwaite (1944) popularized the concept of ET and proposed a model which requires monthly average temperature data only. This model is a simpler model for its data requirement (Alkaeed et al., 2006). The Thornthwaite model is given as **Eq. 6**.

$$ET_{0Trw} = 16\left(\frac{10\,Ti}{I}\right)^{a}\left(\frac{N}{12}\right)\left(\frac{I}{30}\right) \tag{6}$$

$$I = \sum_{i=1}^{12}\left(\frac{Ti}{5}\right)^{1.514} \tag{7}$$

$$a = (492390 + 17920I - 77.1\mathrm{I}^2 + 0.675\mathrm{I}^3) \times 10^{-6} \tag{8}$$

Where, T_i is the mean monthly temperature (°C), N is the mean monthly sunshine hour.

Hargreaves-Samani (1985) model is another temperature based model, which is one of the older ET model introduced by Allen and Hargreaves first (**Eq. 9**). The required data for this model is only measured temperature data (Hargreaves and Allen 2003).

$$ET_{0Hrg} = 0.0023(T + 17.8)(T_{max} - T_{min})^{0.5}R_a \tag{9}$$

Where, T is average air temperature (°C), T_{max} and T_{min} are daily maximum and minimum air temperature, respectively (°C), R_a is daily extraterrestrial radiation (MJ m^{-2} d^{-1}).

The Hamon model is another simple temperature based model that is applicable for estimating ET_0 on monthly or annually basis. According to the Haith and Shoemaker (1987), this model requires only the average number of daylight hours and the saturated vapor pressure (**Eq. 10**) (Haithy and leslie 1987).

$$ET_{0Hom} = \frac{2.1 \times {H_t}^2 e_s}{(T_{Ave} + 273.3)} \quad (10)$$

Where, H_t is the average number of daylight.

The radiation based models are the simplification of the Penman-Monteith model, carried out by Irmak et al. (2003) as expressing a multi-linear regression function that only net radiation (R_n) and solar radiation (R_s) are needed as input data for estimation (Eq. 11 and 12).

$$ET_{0Rn} = 0.489 + 0.289R_n + 0.023 \times T_{Ave} \quad (11)$$

$$ET_{0Rs} = 0.611 + 0.149\ R_s + 0.079 \times T_{Ave} \quad (12)$$

Where, R_n is net radiation (MJ m^{-2} d^{-1}), R_s is solar radiation (MJ m^{-2} d^{-1}).

Finally, the FAO-24 reference crop evapotranspiration (ET_{pan}) was used as indicator to evaluate the performance of the theoretical models. To estimate FAO-24 reference crop evapotranspiration, class-A pan evaporation (E_{pan}) was adjusted by a pan coefficient (k_p) (**Eq. 13**) Allen et al. (1991). k_p was estimated using Snyder model which is given as **Eq. 14**.

$$ET_{pan} = k_p E_{pan} \quad (13)$$

$$k_p = 0.482 + 0.24Ln(F) - 0.000376u_2 + 0.0045RH \quad (14)$$

Where, F is upwind fetch distance of low growing vegetation (m), RH is relative humidity (%), u_2 is wind speed (m s^{-1}).

2.3. Results and Discussion

The difference between ET_{pan} and ET_0 rates was seen mainly in the first period (windy summer). The reasons might be due to the seasonal variation in the climatic condition, and particularly the strong wind speed that prevails in Herat during the summer season, in one hand, and the differences of the models, in the other hand.

2.3.1. Seasonal Variation of the Metrological Variables

The region in a year has four seasons: spring (March-June), summer (June-September), fall (September-December), and winter (December-March). Daily variations in the meteorological variables across the four seasons are shown in **Figure 2-2** from A to D. The daily variations in T, u_2, RH, R_s, R_n is the reason for the daily variation of the ET_0 estimation.

RH ranged from above 10 % to less than 60 % in the spring, above 40 % to less than 80 % in the winter, above 20 % to less than 70 % in the fall. The summer season was characterized by significantly lower humidity of below 30 %. The u_2 rate was higher during the summer compared to the other seasons, by 3.5 m s^{-1} on average. As well as, the T rate was higher in the summer, at more than 30 °C, dropping below 30 °C from the early part of December until the middle of spring. R_n was decreasing by early fall and again increasing from late winter on.

The estimated value of ET_0 were compared with ET_{pan} using the data of 2009. The results shown in Figures 2-3 to 2-8. ET_{0PM} produced closer rate to ET_{pan} throughout the year, however, their rates were almost identical in the period from November to June. In the summer season, and especially from June to November, ET_{pan} gave higher rates than ET_{0PM} (**Figure 2-3**). One of the reasons is the strong "120-day winds" which blows thought the summer season with high speed in Herat province. The difference between the ET_{pan} results and those of the other methods was significantly large in the period approximately from June to November, while in the other months were smaller (**Figures from 2-4** to **2-8**).

The total annual values of ET_0 estimated are shown in **Figure 2-9**. ET_{pan}, ET_{0PM} and ET_{0Hrg} produced higher total annual values compared to the other methods. ET_{0PM}

produced the second highest value of 1,800 mm year^{-1}, while ET_{0RS}, ET_{0Rn}, ET_{0Ham}, and ET_{0Trw} produced lower values, respectively. ET_{0Trw} produced the lowest value below 1,000 mm year^{-1}. Variations in the ET_0 estimation reflect the differences in the variables applied in each method. From the results, ET_{0PM} method can be considered as the useful method for estimating ET_0 in the investigated area.

2.3.2. Relationship Between $\boldsymbol{ET_{pan}}$ And $\boldsymbol{ET_0}$

Brutsaert and Parlange (1998) indicated that, ET_{pan} is often taken as a good indicator for ET_0 evolution. Because all the methods are influenced by some of the same parameters, a linear relationship exists among them. Therefore, Pearson's correlation was used to test the relationship between ET_{pan} and each of the other methods to identify the periods in which correlation was strongest. Pearson's correlation coefficient is often used when measuring the influence of one time-dependent variable on another in bivariate climate time series data (Mudelsee 2003). Here, the selected models were correlated with ET_{pan} in two different periods to identify the seasonal differences. The two periods were separated based on the wind speed.

First period:

The grey triangles in **Figures 2-10 to 2-15** depicts the first period that is from June to September (the windy summer). During this period, no statistically significant correlation was found between ET_{pan} and the other models.

Table 2-2 shows that the p-value of all models were smaller than 0.05 %. The seasonally-based average difference between ET_{pan} and the other models including the standard error estimate (SEE) are shown in **Table 2-2**. The seasonally-based difference between ET_{0PM} and ET_{pan} yielded the smallest as 3.3 mm season^{-1}. The SEE value was yielded the second smallest as 1.9 mm d^{-1}. As it is known, ET_{0PM} requires four different variables this condition might be one of the reasons that this model has good adaptability than the other models.

Second period:

The black round dots in **Figures 2-10 to 2-15** represent the second period that is from October to May characterized by a light wind speed (the fall, spring and winter seasons). In this period, the wind speed is lower than in the first period (the windy summer). All models correlated more strongly to ET_{pan} in this period compared to the first period, and are appropriate for estimating ET_0 in the investigated region.

2.4. Summary

The aim of this study was to contribute in irrigation scheduling by proposing adaptable models that are widely used for estimation of ET_0 in Herat, Afghanistan. Six well-known models, The Penman-Monteith, Hargreaves, Hamon, Thornthwaite, solar radiation based and net radiation based were compared against ET_{pan}. Results showed that, the summer season was characterized by low humidity due to low precipitation, while the wind speed was higher by 3.5 m s^{-1} on average when compared with the other seasons. Temperature was higher in the summer season, dropping in the early days of the fall season and rising again in the middle of the spring season. Net radiation drops by the beginning of the fall season and increases again in the late winter season.

All models produced estimates that were significantly different from those of ET_{pan} in the first period (summer season), with the exception of the ET_{0PM} method. This model had close agreement with ET_{pan}, except in the months from June to November. In the second period (the spring, fall and, winter seasons), all six models produced values close to those of ET_{pan}. This suggests that they are applicable to apply for estimating ET_0 in this period. The total annual ET_0 values estimated by the tested methods ranged from 1,000 to greater than 2,000 mm $year^{-1}$, with ET_{pan}, ET_{0PM} and ET_{0Hrg} producing higher values than the four others, respectively.

None of the six models produced results that were significantly correlated with those of

ET_{pan} in the first period, however, better correlations were found in the second period. The ET_{0PM} method had the best correlation, producing the closest results to those of ET_{pan} in both periods. Based on a SEE calculation and seasonally-based averaged differences, ET_{0PM} also produced the lowest values in the first period.

Figure 2-1 Location of Urdu Khan farm and airport in Herat, Afghanistan.

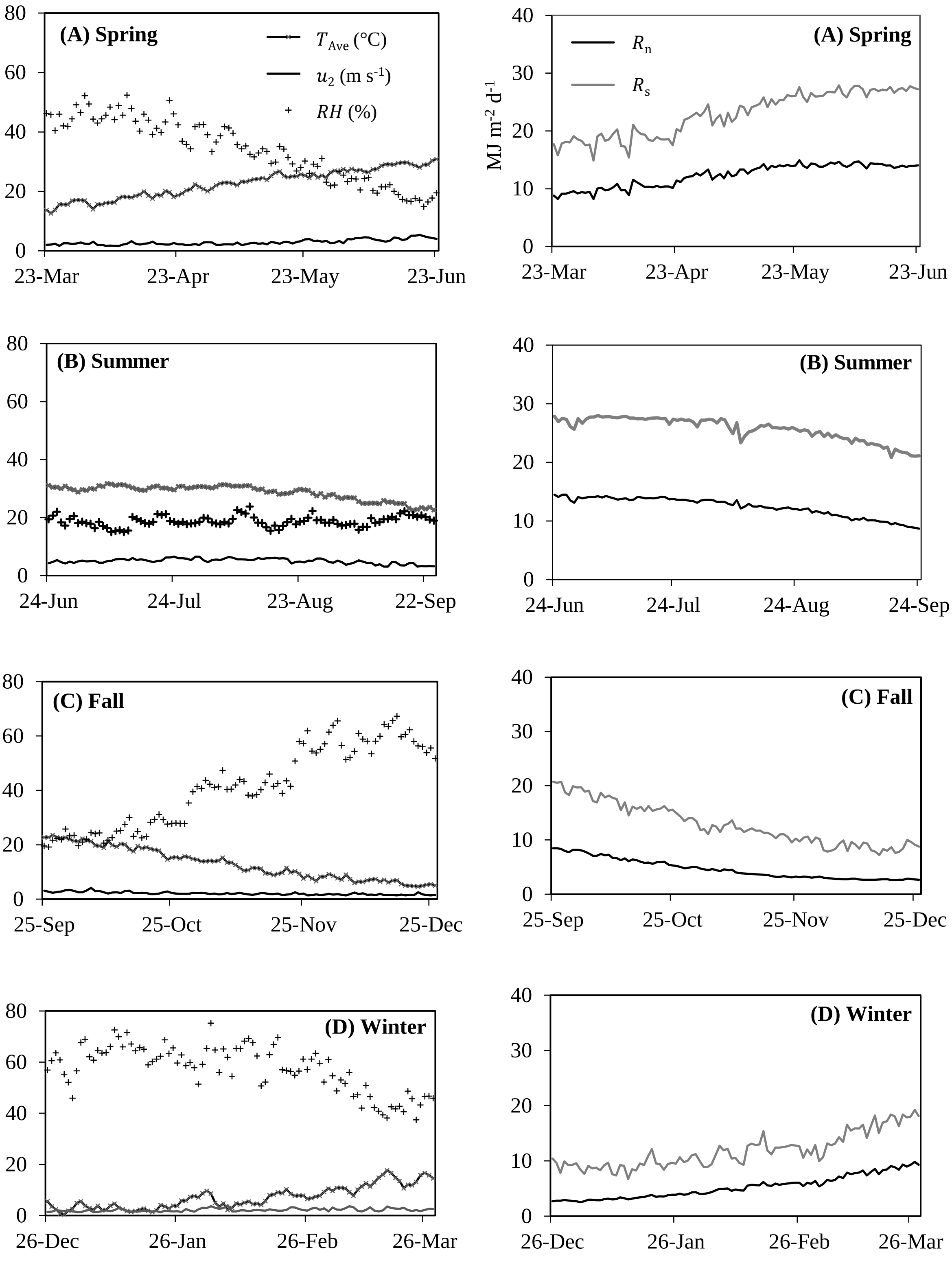

Figure 2-2 Daily average air temperatures, wind speed, relative humidity, net radiation and solar radiation in 2009, (A) spring, (B) summer, (C) fall and (D) winter seasons (Ganji et al., 2017).

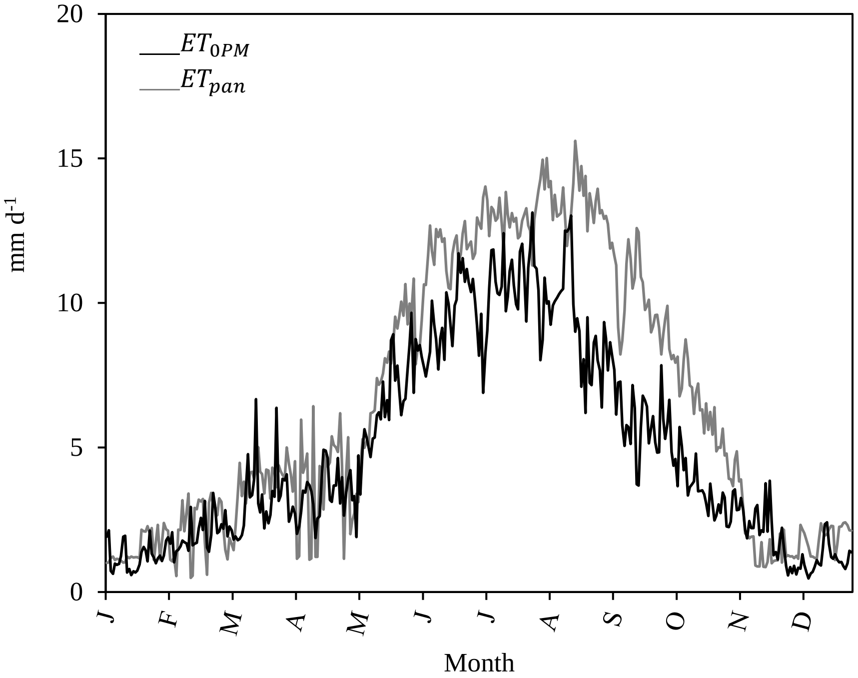

Figure 2-3 Daily average value estimated by ET_{pan} and ET_{0PM}, 2009 (Ganji et al., 2017).

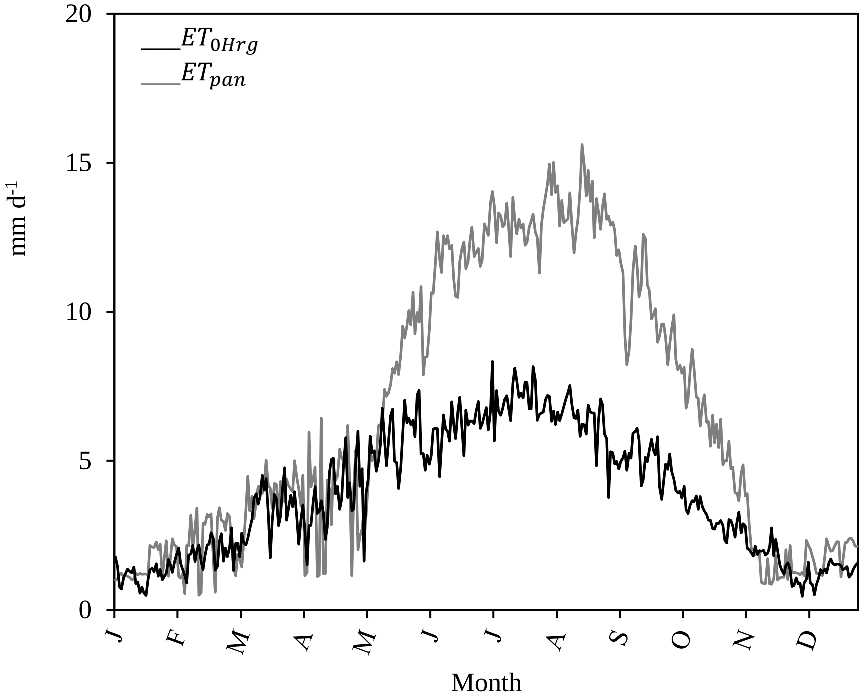

Figure 2-4 Daily average value estimated by ET_{pan} and ET_{0Hrg}, 2009 (Ganji et al., 2017).

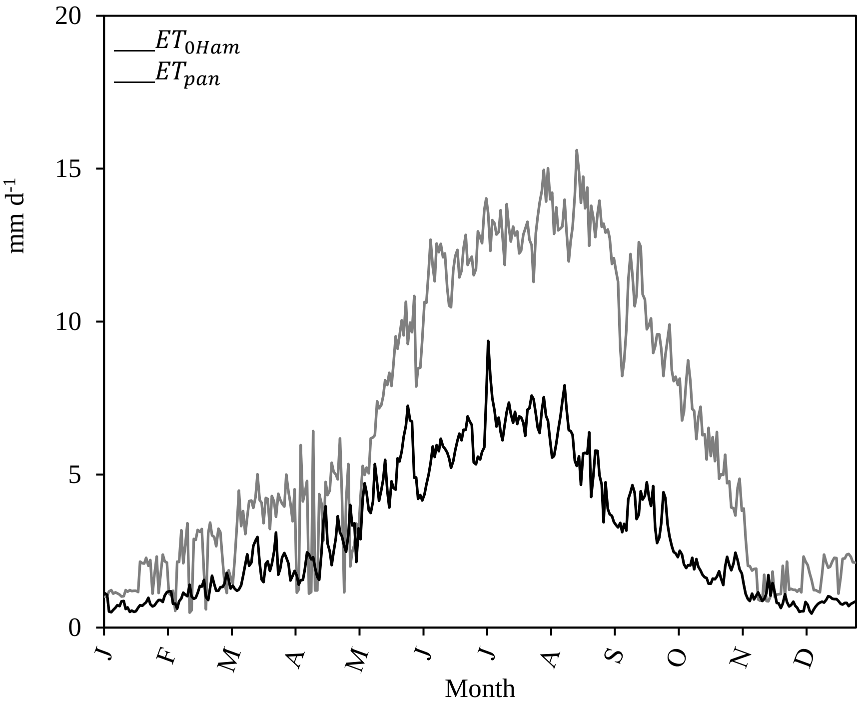

Figure 2-5 Daily average value estimated by ET_{pan} and ET_{0Ham}, 2009 (Ganji et al., 2017).

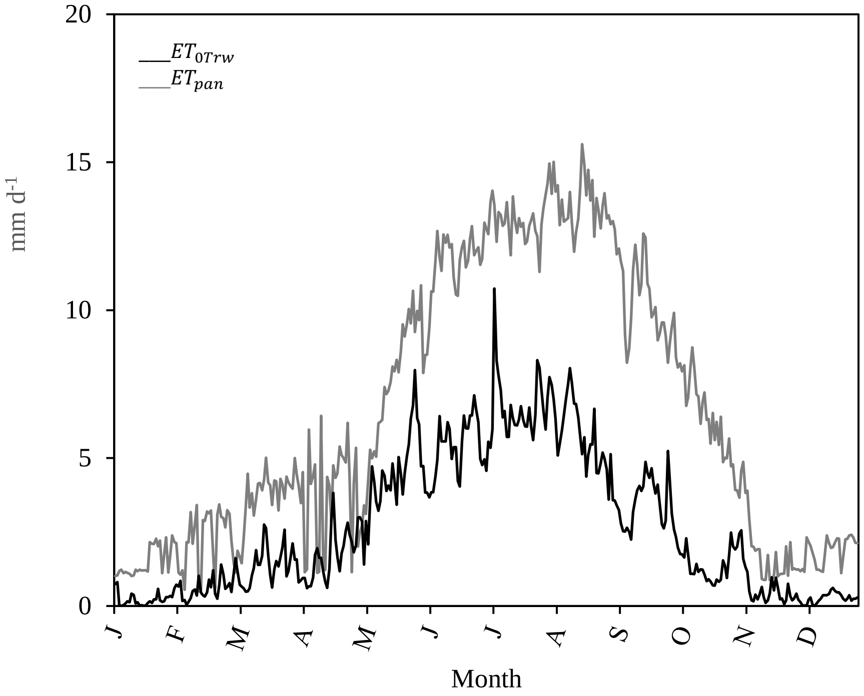

Figure 2-6 Daily average value estimated by ET_{pan} and ET_{0Trw}, 2009 (Ganji et al., 2017).

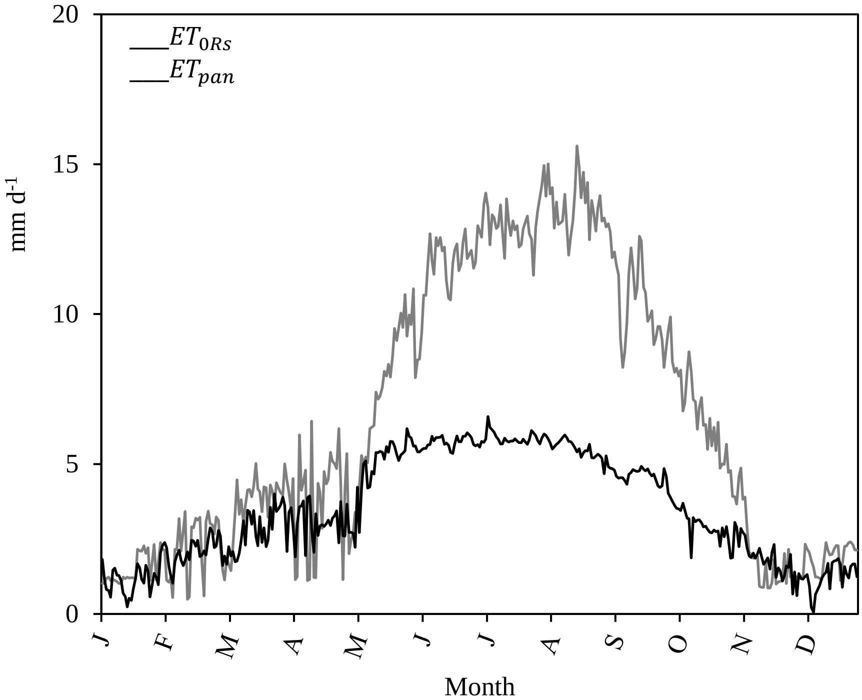

Figure 2-7 Daily average value estimated by ET_{pan} and ET_{0Rs}, 2009 (Ganji et al., 2017).

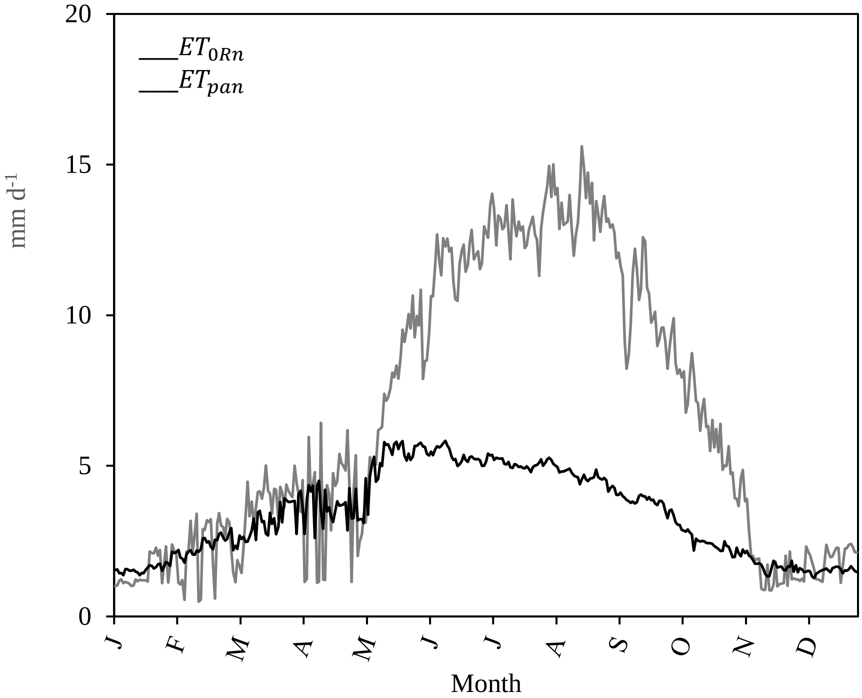

Figure 2-8 Daily average value estimated of ET_{pan} and ET_{0Rn}, 2009 (Ganji et al., 2017).

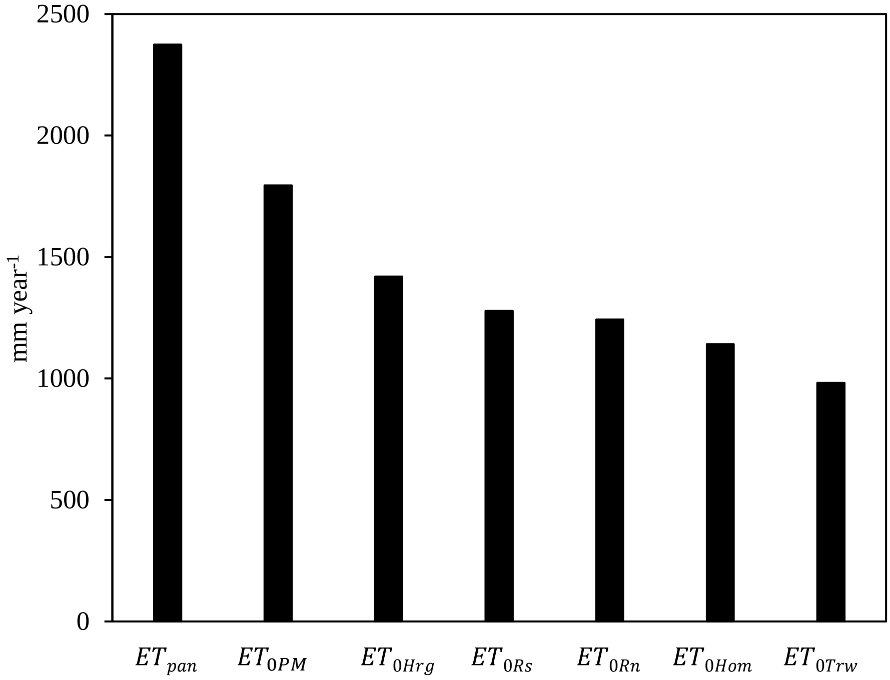

Figure 2-9 Total annual ET_0 estimates given by the different methods based on 2009 (Ganji et al., 2017).

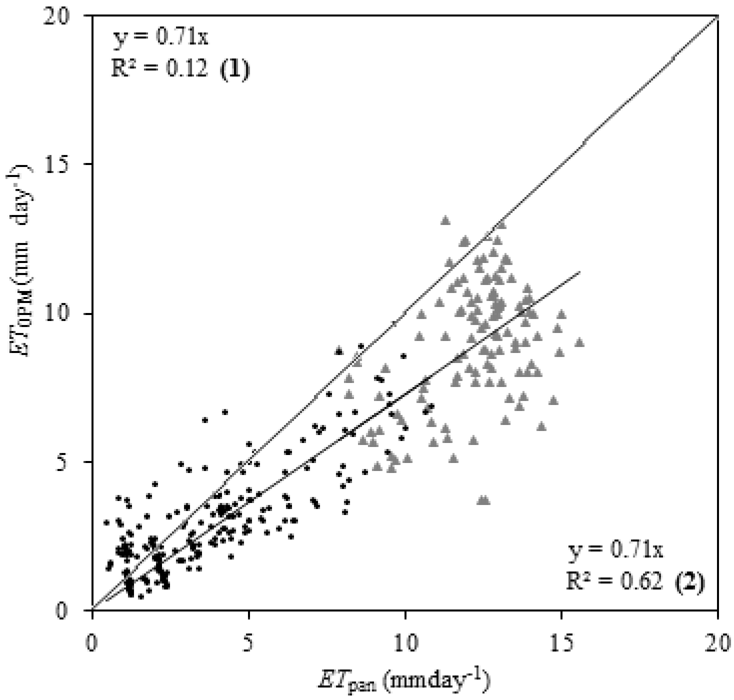

Figure 2-10 Relationship between daily averages estimated by ET_{pan} and ET_{0PM}, 2009 (Ganji et al., 2017).

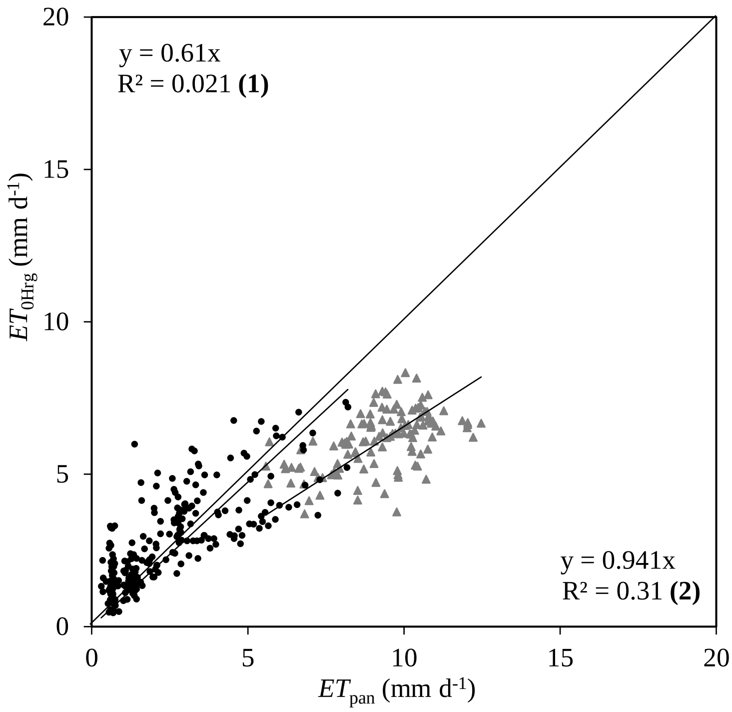

Figure 2-11 Relationship between daily averages estimated by ET_{pan} and ET_{0Hrg}, 2009 (Ganji et al., 2017).

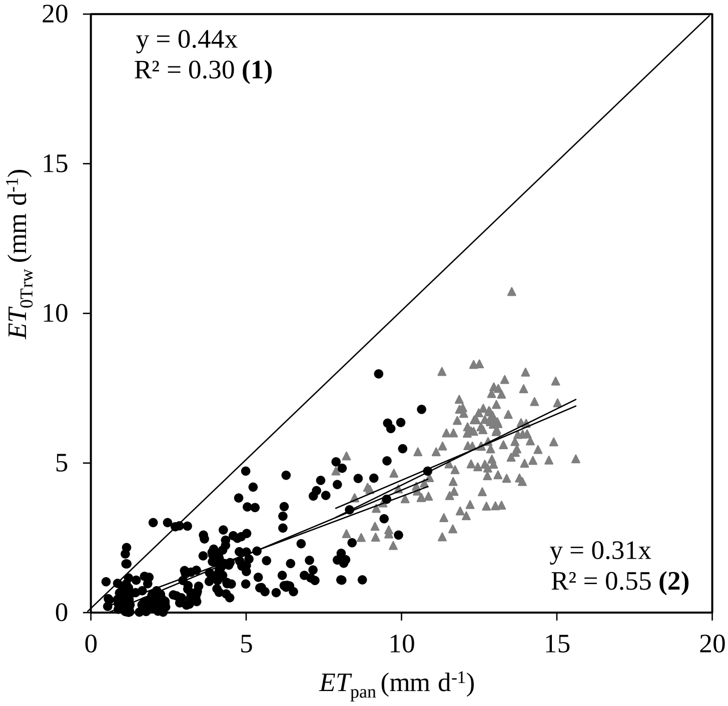

Figure 2-12 Relationship between daily averages estimated by ET_{pan} and ET_{0Trw}, 2009 (Ganji et al., 2017).

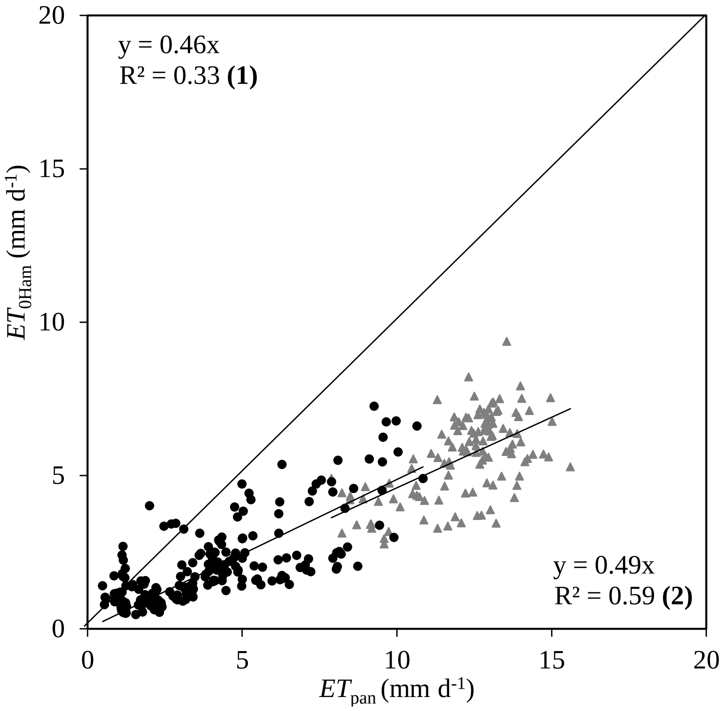

Figure 2-13 Relationship between daily averages estimated by ET_{pan} and ET_{0Ham}, 2009 (Ganji et al., 2017).

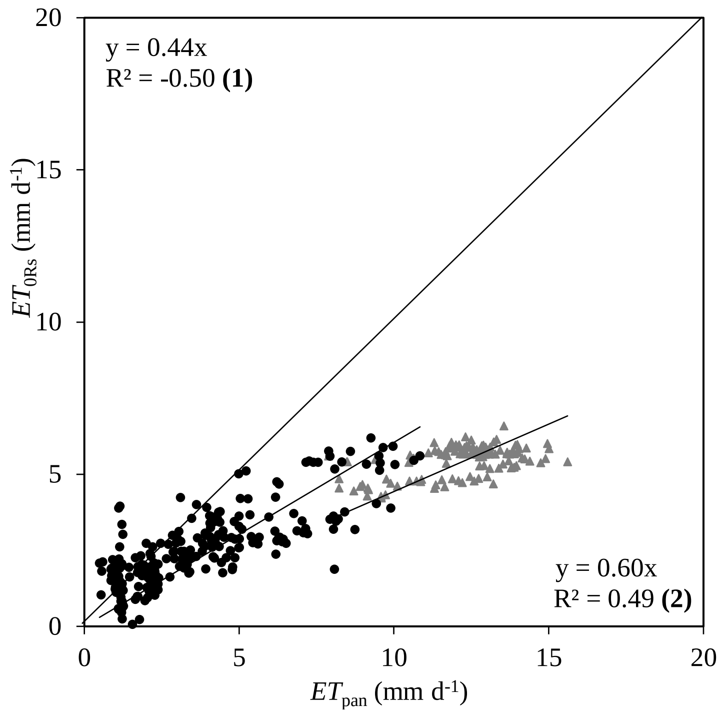

Figure 2-14 Relationship between daily averages estimated by ET_{pan} and ET_{0Rs}, 2009 (Ganji et al., 2017).

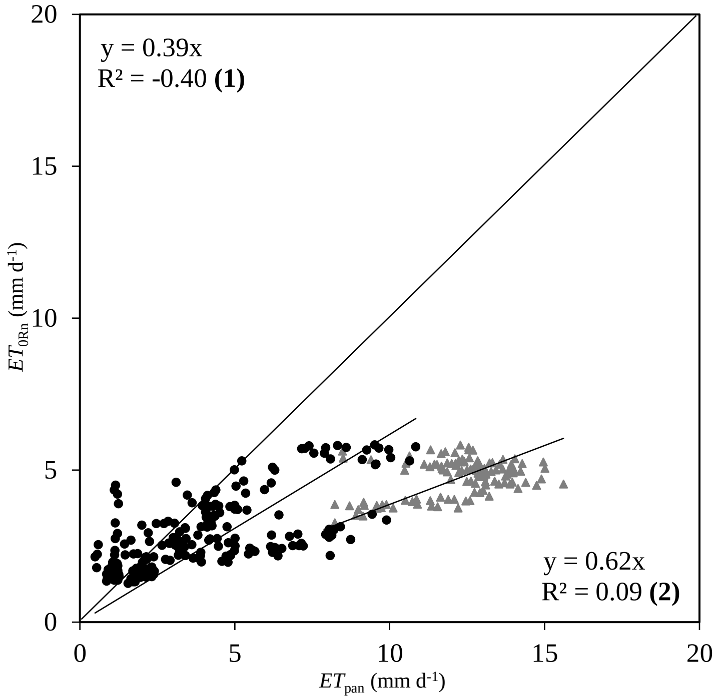

Figure 2-15 Relationship between daily averages estimated by ET_{pan} and ET_{0Rn}, 2009 (Ganji et al., 2017).

Table 2-1 Accessible online database for irrigation planning (Ganji et al., 2017)

Data source	Data kinds	Usage
NCDC (NOAA)	Air temperature, dew point, and wind speed	Basically used data
Weatherspark.com	Cloud cover, wind velocity, air temperature and humidity at the airport.	Supplementary data
Urdu khan Research Farm	Data of E_{pan}, air temperature, sun shine	Supplementary data

Table 2-2 Correlation coefficient, standard error, and seasonally-based average difference in ET_0 (Ganji et al., 2017)

Methods	Coefficients						SEE	$\lvert ** (ET_0) - ET_{pan} \rvert$	**P-value
	**R^2	R^2	**a	a	**n	n	mm d^{-1}	mm d^{-1}	%
Penman-Monteith	0.15	0.67	0.50	0.59	122	243	1.9	3.3	<0.05
R_s-based radiation	0.29	0.66	0.16	0.42	122	243	1.8	6.7	<0.05
R_n- based radiation	0.12	0.51	0.12	0.35	122	243	2.6	7.4	<0.05
(Hamon)	0.33	0.60	0.47	0.42	122	243	2.0	6.6	<0.05
(Hargreaves)	0.28	0.50	0.82	1.58	122	243	2.0	6.0	<0.05
(Thornthwaite)	0.30	0.56	0.51	0.43	122	243	2.0	6.8	<0.05

** indicates the first period (cover summer season).
n indicates the number of days
( ) indicates the temperature based models

Chapter Three

Assessing Reference Evapotranspiration Using Penman-Monteith and Pan Methods in the West Region of Afghanistan

3.1. Background

Spatial distribution of water availability is not uniform among the regions in Afghanistan. Western region, consisting of four provinces such as Herat, Farah, Badghis and Ghour province, is characterized with a semi-arid climate that has low precipitation, as the total precipitation was 345.6 mm in 2009 (Ganji et al., 2014). Many various factors cause agricultural water scarcity in the region, of which the high rate of ET is one of the main factors.

ET_0 in Herat has the highest rate compared with the other cities in Afghanistan, as the daily average value is above 10 mm d^{-1}, especially during the main cropping season (Ganji et al., 2014). One of the factors, among the all other factors which adversely affects ET_0 in the West region, is a persistent winds locally known as “120-day winds”. From the literature it is known that there is a great impact of wind speed in increasing ET_0, which can have profound implications for hydrologic processes and agricultural crop performance (Sabziparvar, 2010).

As explained in Chapter 2, the “120-day winds” usually begin in early June and go on until late September with a great force 7 m s^{-1}, on average (Ganji et al., 2014). This period covers entire of the summer season, which is the main cropping season. According to the measured data in 2009, the precipitation was almost zero during the windy season and daily average temperature was high as 17.5 °C.

Optimal estimation of ET_0 is extremely important as well as needed for calculating the agricultural water volume in the West region. For the ET_0 estimation, many different models have been developed based on their daily performance under the given climatic condition worldwide, of which the Penman-Monteith method (FAO-56PM) was confirmed as the only method offering high accuracy when estimating ET_0 in the West region (Ganji et al., 2017).

Although, the set of Penman equations are the most accurate methods, still there are some studies reporting low performance of these methods when estimating ET_0. Steduto et al.

(1996) conducted a research in Mediterranean locations using lysimeter data. They reported that FAO-56PM underestimated lysimeter data at high rates. Oudin et al. (2005) surprisingly found that the potential evapotranspiration based on the Penman approach seem less advantageous to feed rainfall–runoff models in France, Australia, and the United States. In a study, six well-known models have been examined by Ganji et al. (2017) to estimate ET_0 in the West region of Afghanistan. By considering ET_{pan} as indicator, the FAO-56PM was confirmed as the method closest to ET_{pan}, however, it underestimated ET_{pan}.

Although, the FAO-56PM model produced estimates closest to ET_{pan}, differences emerged between ET_0 and ET_{pan} when compared. In this paper the FAO-56PM equation was examined with the aim to assess the performance of the FAO-56PM method under the climatic conditions of the West region of Afghanistan.

To examine the performance of the FAO-56PM equation pan evaporation data was used. Although, there is no unique approach for model evaluation exists, but the evaporation pan data has been used as an index of evapotranspiration and for estimating lake and reservoir evaporation (Conceicao, 2002). A study in China selected evaporation pan data to evaluate the spatial and temporal difference of monthly reference evapotranspiration using the Penman-Monteith method. The results showed that, pan measurements display a consistent regional pattern and the temporal variability of reference evapotranspiration is much better represented by pan measurements (Chen et al., 2005). Xu (2000) evaluated eight radiation-based equations for determining evaporation using pan evaporation measured data as the indicator at the Changins station in Switzerland.

The pan evaporation is related to the reference evapotranspiration by an empirically derived pan coefficient. The empirically derived coefficient k_p is a correction factor which depends on the prevailing upwind fetch distance, daily average u_2, and RH conditions associated with the sitting of the evaporation pan (Temesgen et al., 2005).

The k_p ranged from 0.35 to 0.85 depending on deferent conditions. Many various equations have been presented for calculating k_p throughout the world, however, those equations cannot compatibly cover the effective environmental factors on k_p, as local estimation is necessary for estimating the accurate value of ET_0. In this study, five different equations were used to estimate k_p. The proposed equations have been tested in different climatic conditions worldwide as they showed different results. Singh et al. (2014) reported that the modified Snyder model has very close agreement with the FAO-56PM and he recommended this model as the best model for computation of ET_0 for a semi-arid region. Sabziparvar et al. (2010) reported that the Snyder and Orang models were the best-fitted models for a warm arid climate. Another study conducted by Conceição (2002) in the Northwest region of the São Paulo State, Brazil reported that ET_0 estimated using k_p determined by the Snyder equation presented the best regression coefficients when compared to the Penman-Monteith method. Gundekar et al. (2008) found that the Snyder (1992) model was the best model for the semi-arid region of India. Sentelhas and Folegatti (2003) indicated that the best k_p models to estimate ET_0 were Cuenca (1989) models, for a semi-arid region in Brazil.

The purpose of this study is to show the critical period for the accurate calculation of ET_0 using the FAO-56PM method for estimating the irrigation water depth.

3.2. Data and Analyzing Method

The West region of Afghanistan (Herat province) was selected as the study area (**Figure 2-1** in Chapter 2). Detail information about the study area was given in Chapter 2.

The climatic data needed for estimating ET_0 was obtained using numerous sources, listed in **Table 2-1** in Chapter 2. As stated earlier in Chapter 2, the main center to record meteorological data is Urdu Khan Research farm. This center being operated by Agricultural, Irrigation and Livestock Department in Herat province of Afghanistan. The center is the only research center in the West region where is used for researches related to agriculture and livestock. The research center was re-equipped with modern devices for measuring the climatic data on 2016. Prior 2016, the station was facing data scarcity as well as low quality data. To reduce the error which would be caused by missing or low-quality data, we used the accessible online database as supplementary for missing and low-quality data.

The FAO-56PM (**Eq. 1**) and the FAO-24 reference crop evapotranspiration (**Eq. 4**) were used to estimate ET_0. k_p was calculated using five different equations such as Cuenca (1989), Allen and Pruitt (1991), Snyder (1992), Orang (1998), and modified Snyder (Grismer et al., 2002). The selected models are described as following:

Cuenca model (1989):

This is a polynomial model functioning based on daily mean relative humidity, wind speed, and upwind-fetch of low-growing vegetation (**Eq. 15**).

$$k_p = 0.475 - 2.4 \times 10^{-4} u_2 + 5.16 \times 10^{-3} RH + 1.18 \times 10^{-3} F - 1.6 \times 10^{-5} RH^2 - 1.01 \times 10^{-6} F^2 - 8 \times 10^{-9} RH^2 \times u_2 - 1 \times 10^{-8} \times RH^2 F \quad (15)$$

where, k_p is the pan coefficient; RH is daily average relative humidity (%), F is up-wind fetch distance of low-growing vegetation (m).

Allen and Pruitt Model (1991):

This model is generally expressed as follows:

$$k_p = 0.108 - 0.000331 u_2 + 0.0422\, Ln(F) + 0.1434 Ln(RH) - 0.000631 \left(Ln(F)\right)^2 Ln(RH) \quad (16)$$

Snyder Model:

In 1992, Snyder found that the Cuenca (1998) model is a complex model which, under different climatic conditions, produces results different from the original coefficient published by Doorenbos and Pruitt (1977). Snyder proposed a simpler to calculate daily k_p

as a function of u_2, RH and F. This model was expressed as follows:

$$k_p = 0.482 + 0.24Ln(F) - 0.000376u_2 + 0.0045(RH) \quad (17)$$

Modified Snyder Model:

The Snyder model was modified based on the original data table by Grismer et al. (2002). The equation is expressed as follows:

$$k_p = 0.5321 + 0.0249\, Ln(F) - 0.00030u_2 + \ 0.0025(RH) \quad (18)$$

Orang Model:

This model was developed by Orang (1998), using interpolation between fetch, and based on the data used to developed FAO-24 k_p. The equation is expressed as follows:

$$k_p = 0.51206 - 0.000321u_2 + \ 0.002889\,(RH) + 0.031886\, Ln(F) - 0.000107\, RH\, Ln(F) \quad (19)$$

3.2.1. Statistical Analysis

A regression analysis was used to determine the accuracy of the results given by the comparison of ET_0 and ET_{pan}. The regression slope (a) was used as the measure of the accuracy, and the coefficient of determination (R^2) was used as the measure of the exactness. Furthermore, according to the suggestion of Jacovides and Kontoyiannis (1995) the root mean square error ($RMSE$), **Eq. 20**, and the mean bias error (MBE), **Eq. 21**, were used to evaluate the difference between ET_0 and ET_{pan}. Smaller $RMSE$ and MBE values indicate better results.

$$RMES = \sqrt{\frac{1}{n}\sum_{i=1}^{n}(ET_{pan} - ET_0)^2} \quad (20)$$

$$MBE = \frac{1}{n}\sum_{i=1}^{n}(ET_{pan} - ET_0) \quad (21)$$

where, $RMES$ is root mean square error (mm d^{-1}), MBE is mean bias error (mm d^{-1}), n is number of data points.

3.3. Results

3.3.1. Daily Variation of Metrological Variables

The climate conditions in the study area was semi-arid with a total annual rainfall of almost 356 mm, occurring in the period from December to April in 2009. Air temperature ranged between 0.5°C to 37°C throughout the year. Daily average temperature increased gradually from January onwards until August. The extremely high average temperature of 29°C was recorded in July, while the lowest value occurred in December (**Figure 3-1a**).

The study area exposed to two different conditions considering wind speed. The wind speed formed two distinguished periods which are called windy and light-windy seasons in this study. **Figure 3-1b** shows the period from June to September, with wind speed ranged between 1.2 to 6.6 m s^{-1} and daily average of 3.5 ms^{-1}. The peak occurred in June at above 6 ms^{-1}. Therefore, the period from June to September is known as the windy season (120-day winds), with relatively strong wind speed. While the rest of the year was exposed to a light wind speed with daily average speed of 1.5 m s^{-1}.

Relative humidity ranged from 7% to 97% entire of the year. The lower daily average rate was recorded in the period from May to November almost 20%, while the extreme lowest rate of below 20 % was recorded during the period from June to August. The highest rate occurred in December (**Figure 3-1c**).

Net radiation was estimated using sunshine data. Net radiation estimated with the highest rate of above 15 MJ m^{-2} d^{-1} in the period of June and July (**Figure 3-1d**).

The E_{pan} data was measured directly at the site. In the period from October to May, the E_{pan} rate was below 5 mm d^{-1} (**Figure 3-1e**). While in the period from June to September the daily average E_{pan} rate ranged from 5 mm d^{-1} to above 15 mm d^{-1} with a peak occurring in August at above 15 mm d^{-1}. **Figure 3-1f** depicts the ET_0 rate which was estimated using FAO-56PM method. The rate of ET_0 was extremely high, above 10 mm d^{-1} during the windy season.

In the West region, in the period from June to September, extreme climatic data out of the experienced range were recorded. The extreme climate conditions means high air temperature, low relative humidity and relatively strong wind speed. While during the rest of the year, they were almost within the normal range.

3.4. Discussion

Daily average ET_{pan} was compared with ET_0, as shown by **Figure 3-2** from. ET_{pan} was measured using different k_p calculated with different models. The ET_{pan} calculated using the modified Snyder k_p was well correlated, with regression coefficient (R^2) value of 0.87, among the explored models. While the sequential performances of the other models were as: Cuenca> Orang>Snyder>Pruitt, as shown in **Figures 3-2** from (a) to (e), respectively.

The statistical indices $RMSE$ and MBE shown in **Figure 3-3a** depicts that the modified Snyder model yielded the smallest total $RMSE$ of 1.7 mm d^{-1} with MBE of 0.8 mm d^{-1} throughout the course of the year. While the sequential error of the other models was: Orang<Cuenca<Snyder<Pruitt. The positive MBE revealed that ET_0 is overestimated throughout the course of the year.

The modified Snyder model was the best to estimate ET_{pan} using E_{pan} data. Other researchers already confirmed this, especially under the semi-arid conditions. Therefore, here in this paper, the ET_{pan} that was produced using the modified Snyder k_p was selected to analyze the difference between ET_0 and ET_{pan}.

The monthly average error produced from the differentiation of ET_0 and the modified Snyder ET_{pan} are shown in **Figure 3-3b**. The higher $RMSE$ of above 1.5 mm d^{-1} occurred in the period from June to September with highest value of above 2.5 mm d^{-1} occurring in July. Although, the order of error was not so small in the rest of the course of the year. However, during the windy season the highest error occurred.

3.4.1. Relationship between Climatic Variables and $RMSE$

To know the effect of the climatic factors on error we used the correlation coefficient (r). During the period from spring to fall season, the rise of temperature which depends on solar radiation is a common phenomenon in those areas exposed to semi-arid conditions. On the other hand, during this period relative humidity reaches its lowest rate. However, in the case of wind rate, such a common sense that the wind rises during the period from spring to fall is not common. This is a typical and unique case, occurring in the west region of Afghanistan and the East part of Iran.

The results showed that, in the period from May to October the rate of E_{pan} and ET_0 were larger with an average value of approximately 7 mm d^{-1} and a peak of above 10 mm d^{-1}. While during the rest of the year the average value was below 5 m d^{-1}. As well, the error from the differentiation of ET_{pan} and ET_0 was getting larger during this period. Experimentally, we found that the error highly correlated with the wind speed. This can be confirmed with the values listed in **Table 3-1**. The u_2 with r value of 0.6 showed the strongest correlation compared to the other three variables. The sequential correlation of other variables was: $T > R_n$ and RH. This implies that the higher the wind speed the larger the ET_0 as well as the difference between ET_0 and ET_{pan}. Therefore, it could be confirmed that this kind of error becomes larger when ET_0 becomes larger than 10 mm d^{-1} in the study region.

3.3. Summary

Optimal estimation of ET_0 is extremely necessary for irrigation scheduling and planning due to the limitation of water resources in the west region of Afghanistan (Herat province).

The rate of ET_0 is extremely high during the main crop-growing season. The high rate of ET_0 is related to the extreme climatic data, measured during the period from June to September. While during the rest of the year, the measured climatic data was within the normal range, and the rate of ET_0 was moderate.

To analyze the error of ET_0, ET_{pan} was selected as an index to make comparisons. At the time when ET_{pan} was calculated, it was found that the modified Snyder method is experimentally best to calculate ET_{pan} nearest to ET_0. Therefore, the difference between ET_0 and ET_{pan} was analyzed. For instance, it was found that wind speed is the most correlated climate data to the differentials of ET_0 and ET_{pan}.

It was confirmed that this kind of error becomes larger when ET_0 becomes larger than 10 mm d^{-1}. Thus, engineers should be careful when calculating ET_0 using the FAO-56PM method, especially in the period of high rate (June to September) in the west region of Afghanistan.

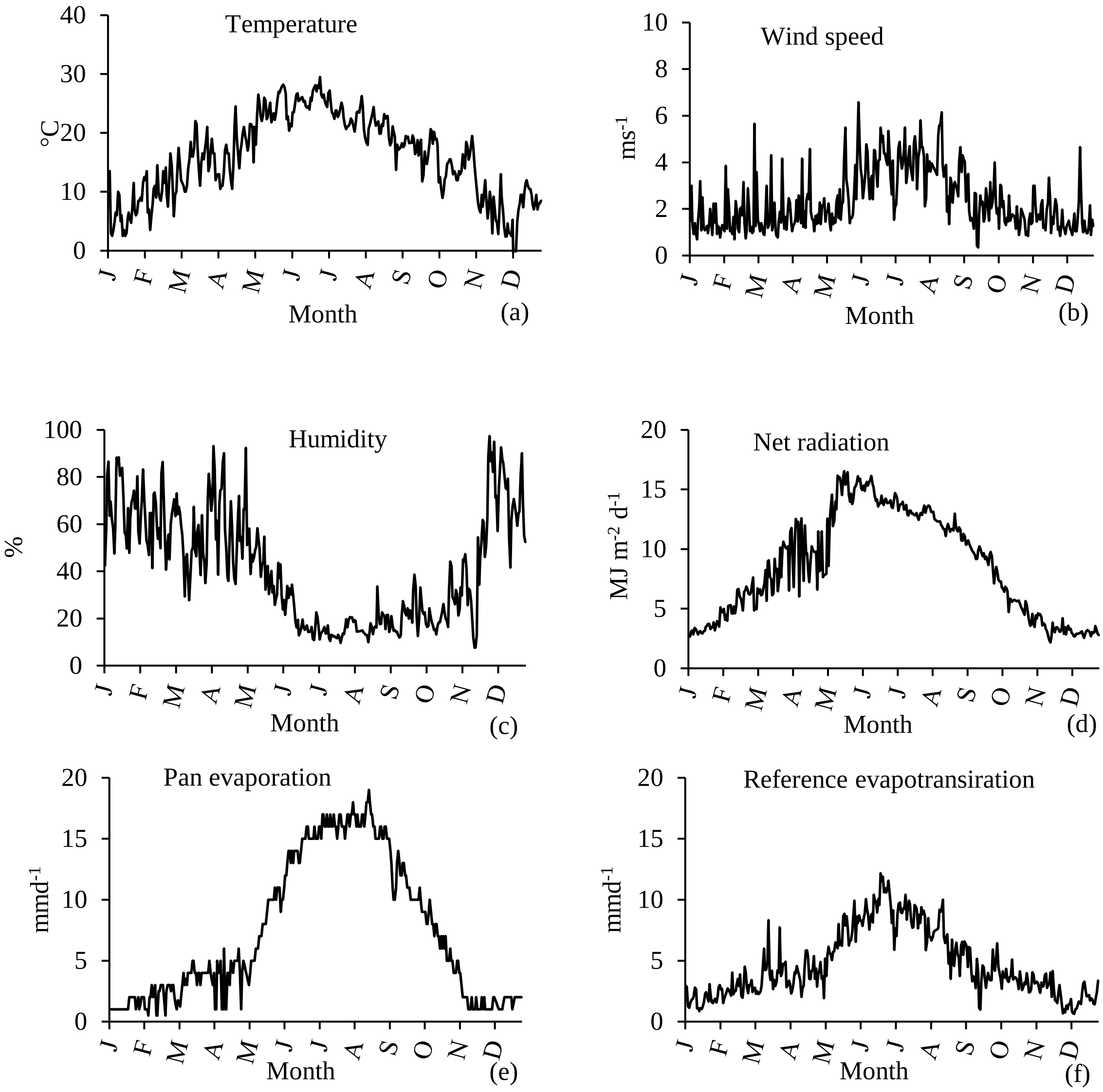

Figure 3-1 Daily average meteorological variables in the period from June to December in a course of a year (a) wind speed, (b) air temperature, (c) relative humidity, (d) net radiation, (e) pan evaporation, and (f) FAO-56PM evapotranspiration (Ganji et al., 2019).

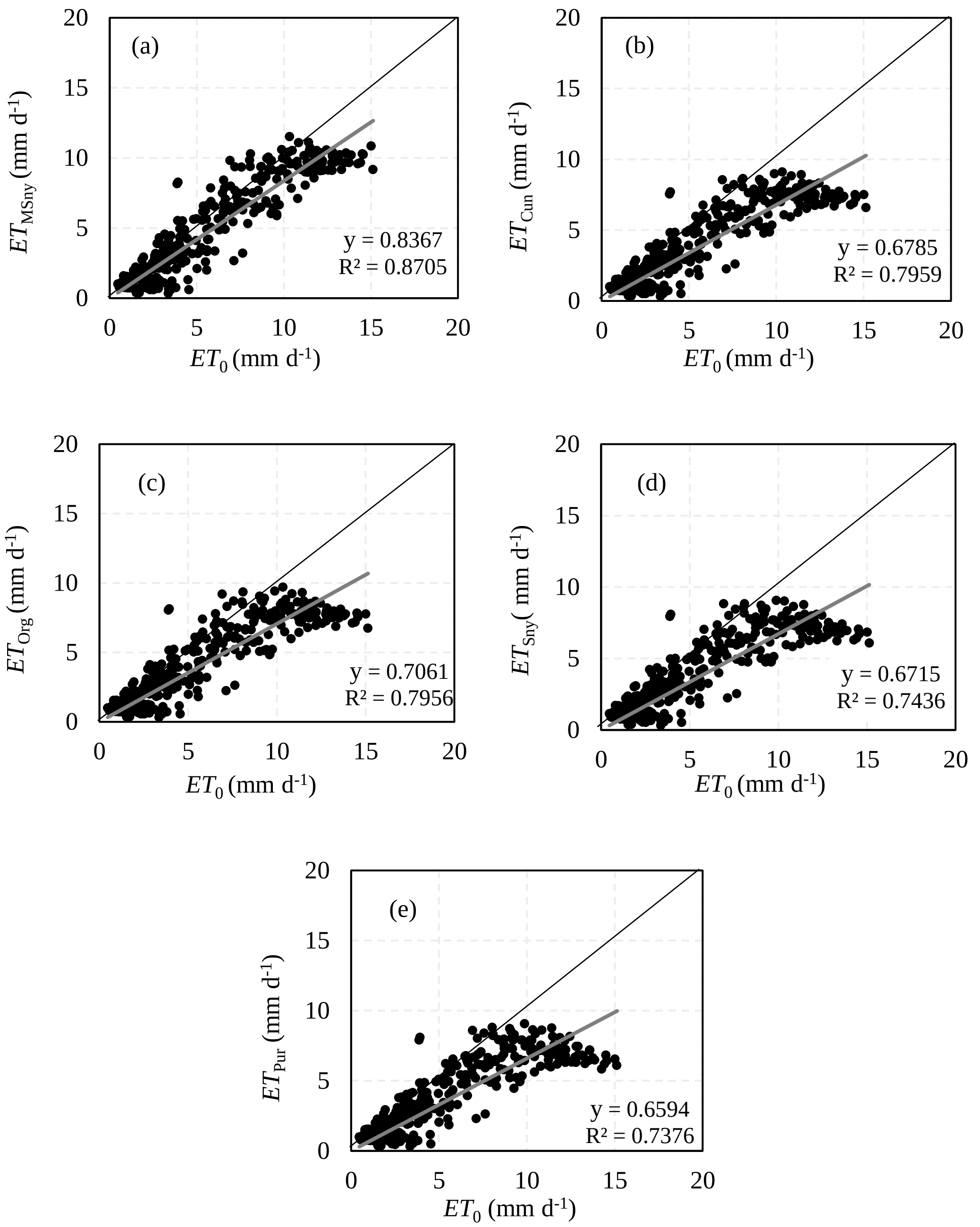

Figure 3-2 Comparison of daily average ET_0 with ET_{pan}; (a) ET_{pan} calculated with k_p proposed by Grismer et al (2002); (b) ET_{pan} calculated with k_p proposed by Snyder; (c) ET_{pan} calculated with k_p proposed by Allen and Pruitt; (d) ET_{pan} calculated with k_p proposed by Cuenca; and (e) ET_{pan} calculated with k_p proposed by Orang (Ganji et al., 2019).

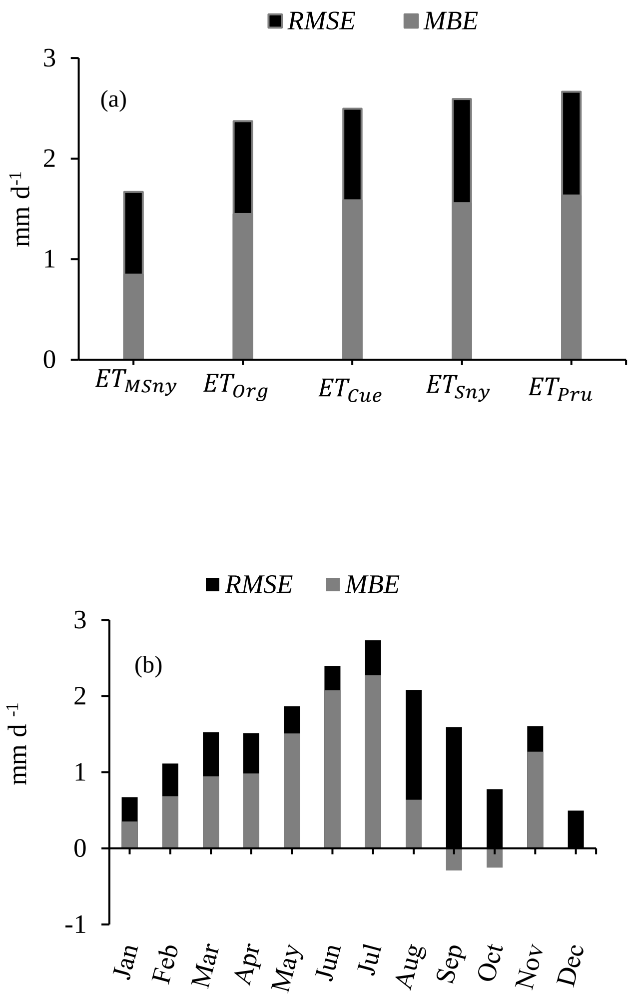

Figure 3-3 Error from (a) total error from the difference between ET_0 and ET_{pan} which were estimated using explorered models; and (b) monthly error from the difference between ET_0 and ET_{pan} which was estimated using the modified Snyder model (Ganji et al., 2019).

Table 3-1 Yearly correlation value between error and climatic variables (Ganji et al., 2019)

Model	$RMSE$ mm d^{-1}	Correlation value (r)			
		u_2	T	RH	R_n
ET_{MSny}	1.7	0.6	0.4	-0.3	0.3

Chapter Four

Assessing the FAO-56 Penman–Monteith Method Using Alternative Data in Semi-arid Conditions

4.1. Background

The FAO-56PM model is a combination method made up of two terms, the radiation and aerodynamic terms. The radiation term depends on the solar radiation, while the aerodynamic term depends on the air temperature, wind speed, and the vapor pressure deficit. However, to estimate ET_0 using Eq. 1, complete input data are required (Allen et al., 1998).

As stated earlier, This model requires data concerning the maximum and minimum temperature (T_{max} and T_{min}, respectively), relative humidity (RH), solar radiation (R_s), and wind speed (u_2) measured two meters above ground level (Allen et al., 1998). While most of the stations around the world, especially in developing countries, are not equipped to supply this complete set of weather variables (Droogers and Allen 2002; Gocic and Trajkovic 2010), this is a severe restriction to the application of the FAO-56PM (Popova, et al., 2006). The geographical-low density of metrological stations in Afghanistan is a big challenge as the metrological variables are often missing or of questionable quality. To overcome this restriction, FAO paper no. 56 supplies procedures that allow the missing variables to be estimated.

The proposed procedures for estimating alternative variables have been tested by many researchers at a variety of locations worldwide and different results have been reported for different climate regimes. Popova et al. (2006) found the procedures proposed by FAO to be accurate when applied in Southern Bulgaria. In a study conducted in Southern Ecuador, Cordova et al. (2015) found that the use of global average wind data had no significant effect on the calculation of ET_0 but that, when the R_s data were missing, the ET_0 calculations became erroneous. A study in Southern Ontario, Canada, conducted by Sentelhas et al. (2010), reported that when RH and u_2 data were missing, the FAO-56PM provided good estimates of ET_0.

The earlier studies have been conducted in various locations worldwide; however, none of them conducted in Afghanistan. It is, therefore, essential to assess the performance of the FAO-56PM when using alternative data with respect to the seasonal variation of the climate conditions in three regions in Afghanistan. Details of the locations explained in **Table 4-1**.

The objectives of this study are as follows:

1) To assess the seasonal climate conditions of the study locations with respect to the climatic variables of T, R_s, RH and u_2 which are necessary to estimate ET_0.
2) To assess the FAO-56PM with alternative R_s, RH and u_2 with respect to the seasonal climate conditions of the study locations.

4.2. Data and Analyzing Method

The climatic data used in the calculation, were provided by automatic weather stations that have recently been launched in the study regions. The stations are operated by the Agriculture Irrigation and Livestock departments in each region. The records were available at two meters above the ground level from April 2016 to March 2017.

The FAO-56PM (**Eq. 1**) was used to estimate daily average ET_0 using complete and alternative data. In this study, the estimation with complete data is abbreviated as ($ET_{0(PM)}$) and those of estimated with alternative data are as ($ET_{0(Alt)}$).When the alternative data of R_s , e_a and u_2 are substituting in **Eq. 1** separately, the $ET_{0(R_s)}$, $ET_{0(e_a)}$ and $ET_{0(u_2)}$ estimations were yielded, respectively.

4.2.1 Alternative Procedure for Estimating Alternative data

In the FAO paper no.56, some procedures are adopted that allow the missing of solar radiation, relative humidity, and wind speed to be estimated. The solar radiation and relative humidity can be estimated using air temperature only, while the missing of wind speed can be substituted by constant global average value of 2 m s^{-1} (Allen et al., 1998). The procedures are described below:

Solar Radiation:

When R_s based on hours of sunshine or direct measured data is missing, Hargreaves' radiation formula as a function of T_{min} and T_{max} is recommended to be substituted the missing data, this is given as **Eq. 6**. Hargreaves' radiation formula assumes that the difference between T_{min} and T_{max} is governed by the daily solar radiation (Hargreaves and Samani 1985). It is abbreviated here in this study as ($R_{s(Alt)}$).

$$R_{s(Alt)} = k_{Rs}\sqrt{T_{\max} - T_{min}}R_a \tag{22}$$

Where, $R_{s(T)}$ is the solar radiation based on temperature (MJ m^{-2} d^{-1}), k_{Rs} is the adjustment coefficient (0.16) for an interior area (ºC$^{-0.5}$), $T_{\max}$ is the maximum air temperature (ºC), T_{min} is the minimum air temperature (ºC), R_a is the extraterrestrial radiation (MJ m^{-2} d^{-1}).

Relative Humidity:

When RH data are unavailable, the actual vapor pressure (e_a) cab be calculated on the assumption that T_{min} is close to T_{dew}, this is given as **Eq.23**. This is useful practically in the humid areas. In arid areas, however, there is often a large difference between T_{min} and T_{dew} (Kimball et al., 1997).

$$e_{a(Alt)} = 0.611e^{\left(\frac{17.27\times T_{min}}{T_{min+273.3}}\right)} \tag{23}$$

Where, $e_{a(Alt)}$ is the actual vapor pressure estimated using T_{min} (kPa).

Wind Speed:

When u_2 data are lacking, two alternative methods are recommended: either the default world average value of u_2 as 2 m s^{-1} is used or u_2 data from a nearby station are used if available (Allen et al., 1998).

4.2.2. Statistical Analysis

In accordance with earlier studies (i.e. Sentelhas P. C. et al., 2010; Cordova et al., 2015; Popova et al., 2006), regression analysis was used to discuss the performance of the $ET_{0(PM)}$ and those estimated using alternative data. The linear coefficient forcing through the origin ($a = 0$). The regression slope (b) was used as the measure of the accuracy, and the coefficient of determination (R^2) was used as the measure of the exactness.

4.3. Results

The seasonal variation of the climatic variables those are necessary to estimate ET_0, shown in **Figure 2-1** from (a) to (d). The similar shape of the time-series data curves of T, R_s and vapor pressure deficit (VPD) were identical with small variation all over the course of the study period in all three locations (**Figure 4-1 from a to c**). The seasonal differences between the locations was seen based on the u_2 rate. From the US weather bureau description, the wind greater 3 m s^{-1} and below 5 m s^{-1} is called gentle-moderate wind speed, while below 3 m s^{-1} can be called light wind speed (**Table 4-2**). Therefore, the study locations were classified in two different categories with respect to the variation of the u_2 rate.

1) Gentle-moderate windy period which was confirmed in Parwan (Central region) where was exposed to gentle-moderate windy season for half year.
2) light wind speed conditions which was confirmed in Samangan and Jalalabad (**Figure 4-1d**). The classification of the locations based on u_2 rate is given in **Table 4-2**.

With respect to the climate conditions of the study locations, ET_0 was estimated using the alternative data of R_s, RH, and u_2, separately in each location. **Figure 4-2a** shows that, the $ET_{0(R_s)}$ was identical to $ET_{0(PM)}$, while $ET_{0(e_a)}$ and $ET_{0(u_2)}$ underestimated $ET_{0(PM)}$, especially in the high rate, in the case of Parwan entire the course of the study period. The rates of $ET_{0(R_s)}$, $ET_{0(e_a)}$ and $ET_{0(u_2)}$ were identical to $ET_{0(PM)}$ in the case of Samangan throughout the study period, depicted in **Figure 4-2b**. The rate of $ET_{0(R_s)}$ and $ET_{0(e_a)}$ were identical to $ET_{0(PM)}$ in the case of Jalalabad, while $ET_{0(u_2)}$ slightly overestimated $ET_{0(PM)}$, especially in the low rate, during the entire study period, shown by **Figure 4-2c**.

4.4. Discussion

To assess the performance of the ET_0 estimation, the plots of estimated $ET_{0(PM)}$ versus those estimated using alternative data in all three study locations are shown in **Figure 4-3** from (a) to (i). The comparison of $ET_{0(PM)}$ versus $ET_{0(R_s)}$ in **Figure 4-3a to c**, shows that $ET_{0(R_s)}$ performed better in all study locations. This is implying that $R_{s(Alt)}$ is effective to be used for estimating ET_0 in semi-arid locations (i.e. Afghanistan).

The comparison in **Figures 4-3d** and **4-3g** shows a weak performance of the $ET_{0(e_a)}$ and $ET_{0(u_2)}$ in the case of Parwan. While their performances were better in the case of Samangan and Jalalabad (**Figures 4-3e to f** and from **4-3h to 4-3i**). The wind speed and VPD are combined as $[u_2 \times VPD]$ in **Eq. 1**. This combination shows if any noise occurs in the VPD calculation, it will become greater with the higher wind speed, this can be the reason of the poor performance of $ET_{0(e_a)}$ in the case of gentle-moderate windy season in Parwan (see **Figure 4-3d**). Thus, the alternative e_a for estimating of RH was not effective in such climate conditions.

The higher rate of ET_0 were produced under the gentle-moderate wind speed condition, while the lower rate were yielded under the light wind speed. Therefore, when deriving ET_0 in locations having a wind speed different from 2 m s^{-1}, using the alternative u_2 would affect the performance of $ET_{0(u_2)}$. This can be the reason that the $ET_{0(u_2)}$ poorly performed in Parwan (**Figure 4-3g**). Hence, the measurement of u_2 is essential in such climate conditions.

4.5. Summary

The ET_0 calculation is needed when determining water requirement of the crop for irrigation scheduling. The FAO-56PM model as a standard model offering high accuracy, which is used widely for estimating ET_0. The high data demand to calculate using this method is a big limitation in locations where are facing with data scarcity such as the case of Afghanistan. When not sufficient, alternative data is used for missing variables. The alternative data of solar radiation, humidity, and wind speed can be obtained from the procedures adopted in FAO paper no. 56. In this study, the performance of the **Eq. (1)** when calculated using alternative data, was assessed with respect to the climate conditions in three different locations in Afghanistan. The results were concluded as:

1) We could classify the study locations based on the seasonal variations in u_2 rate as following: One, Parwan in the central region can be focused as the location includes gentle-moderate windy season. Two, Samangan in the Northern region and Jalalabad in the Eastern region can belong to the locations with light wind speed only.
2) The estimations of ET_0 when computed using alternative data of solar radiation, humidity, and wind speed, separately, were found as follows: The measurement of RH and u_2 are very essential under gentle-moderate wind speed conditions. The performance of $ET_{0(e_a)}$ and $ET_{0(u_2)}$ were weak in the Parwan location that include the gentle-moderate windy season. The lack of R_s did not affect the ET_0 estimates at all, as $ET_{0(R_s)}$ performed better under all seasons.

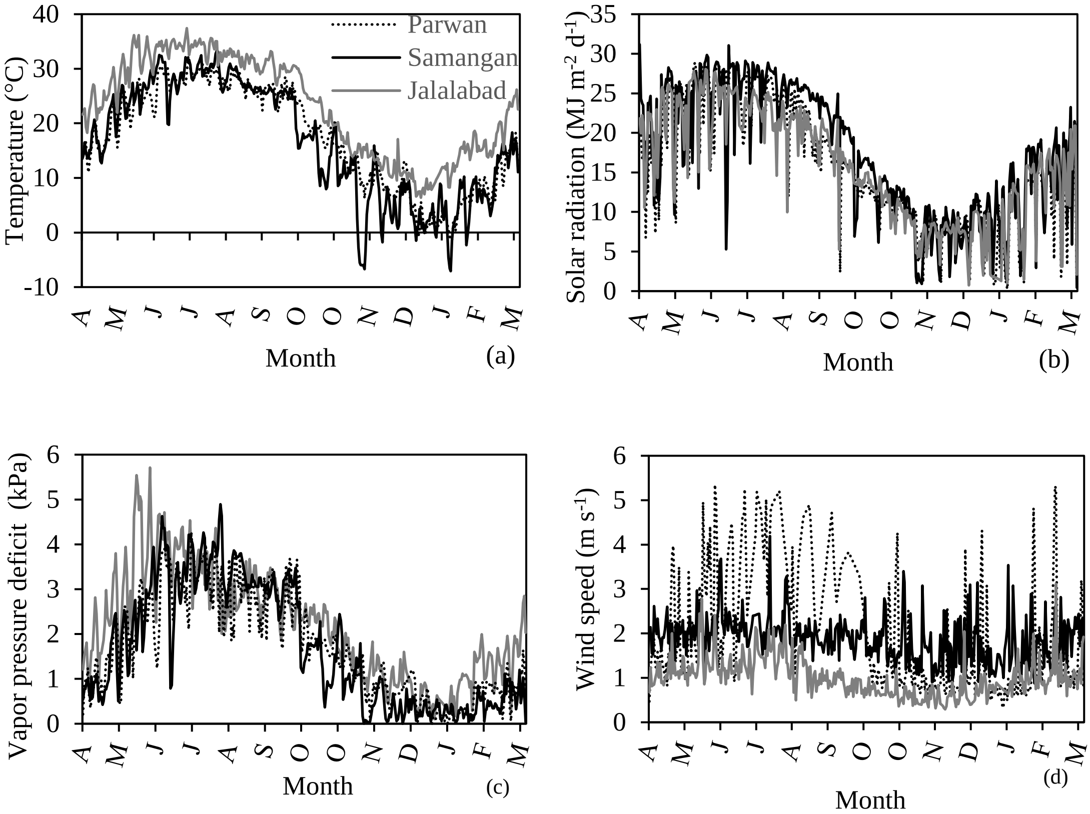

Figure 4-1 Daily average measurement of (a) temperature, (b) solar radiation, (d) vapor pressure deficit, and (d) wind speed (2016. 4 ~ 2017. 3) (Ganji et al., 2018).

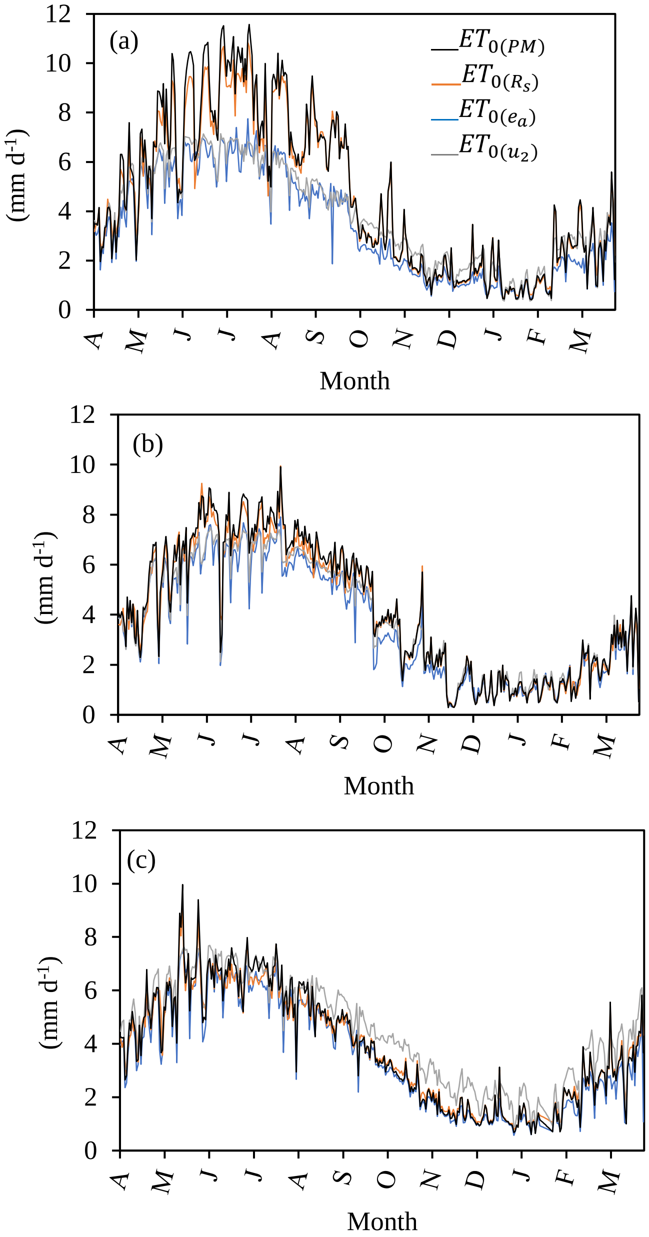

Figure 4-2 Daily average estimation of $ET_{0(PM)}$ and those estimated using alternative data (a) Parwan, (b) Samangan and (c) Jalalabad (2016. 4 ~ 2017. 3) (Ganji et al., 2018).

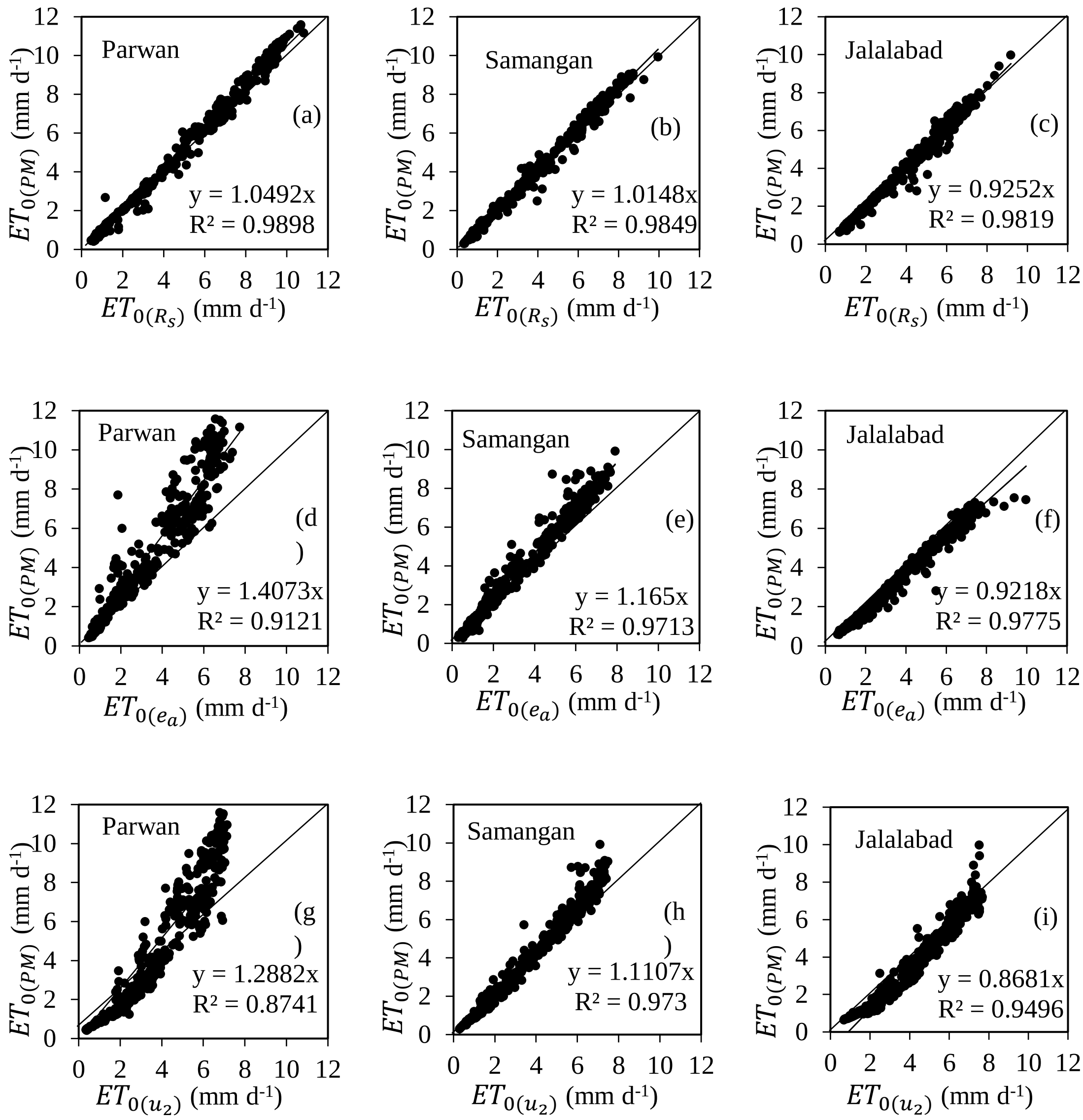

Figure 4-3 Comparison between $ET_{0(PM)}$ and those of $ET_{0(Alt)}$ (Ganji et al., 2018).

Table 4-1 Station's location, coordinates, and elevations (Ganji et al., 2018)

Location's Name	Regions	Latitude (N)	Longitude (E)	Elevation (m)
Parwan	Central	35° 04′	69° 18′	1,573
Samangan	North	35° 83′	67° 78′	959
Jalalabad	East	34° 25′	70° 28′	580

Table 4-2 Seasonal climatic conditions with respect to the wind speed by US description (Ganji et al., 2018)

Locations	Seasonal climate conditions
Parwan	Gentle-moderate wind speed (5m s^{-1}>u_2>3m s^{-1} until Oct) and Lite wind speed (u_2<3m s^{-1} after Oct)
Samangan	Light wind speed (u_2<3m s^{-1})
Jalalabad	Light wind speed (u_2<3m s^{-1})

Chapter Five

Error propagation approach for estimating root mean square error of the reference evapotranspiration when estimated with alternative data

5.1. Background

The validity of $ET_{0(Alt)}$, when estimated with alternative data, has been tested by several researchers in a variety of climate conditions worldwide, using statistical indices such as root mean square error ($RMSE$) and regression analysis (Popova et al., 2006; Jabloun et al., 2008; Sentelhas et al., 2010; Cordova et al., 2015).

For confirming the validity of $ET_{0(Alt)}$, it is essential to calculate $RMSE$; lower values of $RMSE$ indicate better validity. However, neither $RMSE$ or the regression analysis specify the source of error in the ET_0 model when estimating with alternative data. Specifying the source of error in the ET_0 model when estimating with alternative data is very useful for future improvements of the model. The error propagation approach is designed to specify the effect of the alternative data's uncertainty on the error of a function in order to provide an accurate estimation of a function's error. Furthermore, to get the $RMSE$ both ET_0 with complete data set ($ET_{0(St)}$) and $ET_{0(Alt)}$ are needed. While by using the error propagation approach, $RMSE$ can be estimated without using $ET_{0(St)}$.

In this study, the applicability of the theoretical error propagation approach was examined both for calculating $RMSE$ and for specifying the source of error in the model equation. It is expected that errors in ET_0 will be reduced in the future by improving meteorological data obtained using alternative proposals or by improving the Penman-Monteith formula. These two improvements correspond to the two components that constitute the theoretical expression of error propagation. Therefore, it is possible to effectively discuss the effect of improvement using the error propagation theoretical formula. Furthermore, by using this approach, it is possible to estimate $RMSE$ for confirming the validity of $ET_{0(Alt)}$ without using $ET_{0(St)}$.

The objectives of this study are as follows:

1) To compare $ET_{0(St)}$ and $ET_{0(Alt)}$ for confirming the validity of alternative data in the ET_0 estimation.

2) To estimate $RMSE$ using error propagation approach.

3) To specify the source of error in the ET_0 equation when estimating with alternate data.

5.2. Data and Analyzing Method

In this study, metrological data were obtained from the Automated Meteorological Data Acquisition System (AMeDAS), which is a collection of automatic weather stations (AWSs) run by the Japan Metrological Agency (JMA) for automatic observation of precipitation, wind direction and speed, temperature and sunshine duration to support real-time monitoring of weather conditions with high temporal and spatial resolution. JMA began operating the AMeDAS system at average intervals of 17 km nationwide. The data in this study correspond to 48 different locations in 45 prefectures of Japan over a 30-year period from 1988 to 2017. The study locations are numbered from 1–48 in **Figure 5-1**; the corresponding geographical coordinate points are listed in **Table 5-1**. The measured variables T, n, RH and u_2 are needed to estimate $ET_{0(st)}$. The average values of measured variables and the estimated values of R_s and actual vapour pressure (e_a) for each location are listed in **Table 5-1**.

The FAO-56PM (**Eq. 1**) was estimated with both set of data, the measured and alternative, in each location to assess the validity of $ET_{0(Alt)}$. According to the FAO methodology, **Eq. 1** can be calculated with alternative data of solar radiation ($ET_{0(R_s)}$) (**Eq. 24**), alternative actual vapor pressure ($ET_{0(e_a)}$) (**Eq. 25**) (relative humidity is corresponding to actual vapor pressure in the FAO-56PM equation), and alternative wind speed ($ET_{0(u_2)}$) (**Eq. 26**). The procedures allowing the alternative data to be estimated, were described in Chapter 3.

$$ET_{0(u_{2(Alt)})} = \frac{0.408\Delta(R_n - G) + \gamma \frac{900}{T + 273} u_{2(Alt)}(e_s - e_a)}{\Delta + \gamma\left(1 + 0.34u_{2(Alt)}\right)} \tag{24}$$

$$ET_{0(e_{a(Alt)})} = \frac{0.408\Delta(R_n - G) + \gamma \frac{900}{T + 273} u_2\left(e_s - e_{a(Alt)}\right)}{\Delta + \gamma(1 + 0.34u_2)} \tag{25}$$

$$ET_{0(R_{s(Alt)})} = \frac{0.408\Delta(R_n - G) + \gamma \frac{900}{T + 273} u_2(e_s - e_a)}{\Delta + \gamma(1 + 0.34u_2)} \tag{26}$$

5.2.1. Statistical Analysis

As stated in Chapter 4, In accordance with earlier studies (i.e. Sentelhas P. C. et al., 2010; Cordova et al., 2015; Popova et al., 2006), regression analysis was used to assess the performance of $ET_{0(st)}$ and $ET_{0(Alt)}$. The linear coefficient forcing through the origin ($a = 0$), used as the measure of the accuracy, and the coefficient of determination (R^2) was used as the measure of the exactness. The agreement between $ET_{0(st)}$ and $ET_{0(Alt)}$ was assessed using $RMSE$ given as **Eq. 27**. The $RMSE$ is the square root of the variance of the residuals. It indicates the absolute fit of the model to the data—how close the observed data points are to the model's predicted values. $RMSE$ is one of the three statistics which are used in ordinary least squares regression to evaluate model fit.

$$RMSE_{(Alt)} = \sqrt{\frac{1}{m}\sum_{i=1}^{m}(ET_{0(Alt)i} - ET_{0(st)i})^2} \tag{27}$$

where, $RMSE_{(Alt)}$ is the root mean square error (mm d^{-1}), $ET_{0(st)}$ is the correct reference evapotranspiration calculated using measured data (mm d^{-1}), $ET_{0(Alt)}$ is the reference evapotranspiration calculated using alternative data (mm d^{-1}), i is the suffixes of each data, m is the total data number. In this paper, m of 360 was applied as an example that includes 12 months for 30 years.

To calculate the slope, **Eq. 1** is transformed to **Eq. 29**. In this equation the components such as R_s, e_a and u_2 are independent variables, while those of c_1 to c_8 do not include R_s, e_a nor u_2 . The first and second component in **Eq. 28** are given by **Eq. 30** and **31**, respectively.

The error propagation approach is designed to quantify the effect of variables' uncertainty on the error of a function to provide an accurate estimation of a function's error. When the ET_0 by FAO-56 PM is estimated with alternative data, the error of the alternative data should be propagated to the error of ET_0. This is because the resulting output is a function of the input (Gerard, 1998). Therefore, in this study, obtaining the error of ET_0 using this approach, given as **Eq. 28**, was attempted. The approach consists of two components, in which the slope of the function is the derivative of ET_0 with respect to the variables. To calculate the slope, **Eq. 1** is transformed into **Eq. 29**. In **Eq. 29**, components such as R_s, e_a and u_2 are independent variables, while c_1 to c_8 do not include R_s, e_a nor u_2. The first and second components in **Eq. 28** are given by **Eq. 30** and **31**, respectively.

$$\Delta ET_{0(Alt)} = \left(\frac{\Delta ET_0}{\Delta x}\right)\Delta x \tag{28}$$

$$ET_0 = \frac{c_3 R_s - (c_4 - c_5\sqrt{e_a})(c_6 R_s - c_7) + c_8 u_2 (e_s - e_a)}{c_1 + c_2 u_2} \tag{29}$$

$$\frac{\Delta ET_0}{\Delta x} = \sqrt{\frac{1}{m}\sum_{i=1}^{m}\left(\frac{\partial ET_0}{\partial x}\right)_i^2} \tag{30}$$

$$\Delta x_{(Alt)} = \sqrt{\frac{1}{m}\sum_{i=1}^{m}\left(x_{(st)i} - x_{(Alt)i}\right)^2} \tag{31}$$

where, c_1 is given by $\Delta + \gamma$, c_2 is given by 0.34γ, c_3 is given by $0.408\Delta(1-\alpha)$, c_4 is given by $0.34\times0.408\Delta\sigma(T_{max} + T_{min}) \div 2$, c_5 is given by $0.14\times0.408\Delta\sigma(T_{max} + T_{min}) \div 2$,

c_6 is given by $1.35 \div R_{so}$, c_7 is equivalent to 0.35, c_8 is given by $900\gamma \div (T_{Ave} + 273)$, ΔET_0 is the average error of reference evapotranspiration (mm d^{-1}), x is the independent variable (x can be R_s, e_a or u_2), $\Delta x_{(Alt)}$ means the order of the difference between the measured correct data $x_{(st)}$ and the alternative variable $x_{(Alt)}$, i is the suffixes of each data, m is the total data number.

5.3. Results

In order to assess the validity of the alternative data in ET_0 estimation, the FAO-56PM equation was calculated with both sets of data, measured and alternative, in all study locations. The average estimation of $ET_{0(st)}$ and those of the $ET_{0(R_s)}$, $ET_{0(e_a)}$ and $ET_{0(u_2)}$ are shown in **Figure 5-2**. The highest value was yielded by $ET_{0(R_s)}$ and followed by $ET_{0(e_a)}$ and $ET_{0(u_2)}$, respectively in the second and third positions.

The relationship between $ET_{0(\mathrm{st})}$ and the models were significant, as $ET_{0(u_2)}$ had the strongest relationship ($a = 0.97$ and $R^2 = 0.97$), while $ET_{0(e_a)}$ and $ET_{0(R_s)}$ ranked second and third, respectively, **Table 5-2**. The agreement between $ET_{0(st)}$ and the models was confirmed using $RMSE$ and ΔET_0, as depicted in **Figure 5-3**. The highest average $RMSE$ values were from $RMSE_{(R_s)}$ (0.34 mm d^{-1}) followed by $RMSE_{(e_a)}$ (0.20 mm d^{-1}) and $RMSE_{(u_2)}$ (0.13 mm d^{-1}).

The relationship between $RMSE_{(Alt)}$ and $\Delta ET_{0(Alt)}$ is depicted in **Figures 5-4 to 5-6**. **Figure 5-4** shows plots of $RMSE_{(R_s)}$versus $\Delta ET_{0(R_s)}$. The values of $R^2 = 0.96$ and $k = 0.92$ indicate a significant relationship with good proportionality among them. The plots of $RMSE_{(e_a)}$ versus $\Delta ET_{0(e_a)}$ demonstrate a significantly strong relationship and proportionality between them, with an R^2 value of 0.94 and $k = 0.92$, as shown in **Figure 5-5**. **Figure 5-6** depicts the plots of $RMSE_{(u_2)}$ against $\Delta ET_{0(u_2)}$. The values of $RMSE_{(u_2)}$

and $\Delta ET_{0(\mathrm{u}_2)}$ were the smallest. On the other hand, the values of $R^2 = 0.96$ and the proportionality coefficient k =0.94 confirm the best proportionality out of the cases studied.

The values shown in **Table 5-3** relate to the derivative of ET_0 with respect to the variables (slope) and the variable's uncertainty. In the cases of R_s and u_2, slope is larger compared to the variables' uncertainty, while in the case of e_a it is smaller.

5.4. Discussion

The applicability of the error propagation approach for estimating $RMSE$ was examined using the data from 48 different locations for 360 months in Japan. The results confirmed that this is a good choice for estimating $RMSE$ when confirming the validity of the alternative data in a region.

Comparing $ET_{0(Alt)}$ against $ET_{0(st)}$ confirms the validity of $ET_{0(Alt)}$ in **Figure 5-2**. $ET_{0(R_s)}$ was the largest among the alternatives compared to the $ET_{0(st)}$. On the other hand, the $RMSE_{(R_s)}$ and $\Delta ET_{0(R_s)}$ had the largest values, showing weaker agreement between $ET_{0(R_s)}$ and $ET_{0(st)}$ in **Figure 5-3** compared to $ET_{0(u2)}$ and $ET_{0(Rs)}$. The best agreement was obtained between $ET_{0(u_2)}$ and $ET_{0(st)}$, shown in **Figure 5-2**. The values of $RMSE_{(u_2)}$ and $\Delta ET_{0(\mathrm{u}_2)}$ were the lowest and very close to each other.

Confirming agreement between the estimations is difficult without using $ET_{0(st)}$. By considering $ET_{0(st)}$ the results for the $ET_{0(Alt)}$ estimation demonstrate the relationship shown in **Eq. 32**. The same relationship existed in the difference between $ET_{0(Alt)}$ and $ET_{0(st)}$, as shown in **Eq. 33**. Interestingly, a similar relationship could be confirmed in the case of $RMSE_{(Alt)}$ and $\Delta ET_{0(Alt)}$, as shown in **Eq. 34 and** 35, respectively. From this result, $\Delta ET_{0(Alt)}$ can be expected to be proportional to $RMSE_{(Alt)}$.

$$ET_{0(Rs)} > ET_{0(u2)} > ET_{0(st)} > ET_{0(ea)} \tag{32}$$

$$\left|ET_{0(R_s)} - ET_{0(St)}\right| > \left|ET_{0(e_a)} - ET_{0(St)}\right| > \left|ET_{0(u_2)} - ET_{0(St)}\right| \tag{33}$$

$$RMSE_{(R_s)} > RMSE_{(e_a)} > RMSE_{(u_2)} \tag{34}$$

$$\Delta ET_{0(R_s)} > \Delta ET_{0(e_a)} > \Delta ET_{0(u_2)} \tag{35}$$

The order of the difference of $\left|RMSE_{(R_s)} - \Delta ET_{0(R_s)}\right|$ was the largest followed by those of $\left|RMSE_{(e_a)} - \Delta ET_{0(e_a)}\right|$ and $\left|RMSE_{(u_2)} - \Delta ET_{0(u_2)}\right|$, as shown in **Eq. 36**.

$$\left|RMSE_{(R_s)} - \Delta ET_{0(R_s)}\right| > \left|RMSE_{(e_a)} - \Delta ET_{0(e_a)}\right| > \left|RMSE_{(u_2)} - \Delta ET_{0(u_2)}\right| \tag{36}$$

The order of the difference between $RMSE_{(u_2)}$ and $\Delta ET_{0(\mathrm{u}_2)}$ was very small, as shown in **Figure 5**-3. However, the difference was slightly higher in the case of $RMSE_{(R_s)} - \Delta ET_{0(R_s)}$ and $RMSE_{(e_a)} - \Delta ET_{0(e_a)}$. In **Figures 5-4 to 5-6** they show high R^2 and each plot seems to be located on the solid line of proportionality. This kind of proportionality was unexpected from each equation. Based on this experience, we suggest that $RMSE$ will be expressed as $RMSE_{(R_s)} = 1.21\ \Delta ET_{0(R_s)}$ and $RMSE_{(e_a)} = 0.87\ \Delta ET_{0(e_a)}$, shown in **Figures 5-4** and **5-5**, respectively. From the results in **Figures 5-4** to **5-6**, it will be possible for us to predict $RSME$ as ΔET_0 in the range of almost 10% error in the three cases, shown in **Eq. 37 to 39**. These kinds of equations may be helpful for confirming the validity of $ET_{0(Alt)}$ in those areas where the $RMSE$ is difficult to estimate due to the lack of all kinds of measured data.

$$RMSE_{(R_s)} = 1.21\Delta ET_{0(R_s)} \qquad (R^2 = 0.96) \tag{37}$$

$$RMSE_{(e_a)} = 0.87\Delta ET_{0(e_a)} \qquad (R^2 = 0.94) \tag{38}$$

$$RMSE_{(u_2)} = 0.94\Delta ET_{0(u_2)} \qquad (R^2 = 0.96) \tag{39}$$

The values shown in **Table 5-3** indicate that the error in the ET_0 estimation is related to two components. The first is the derivative of ET_0 with respect to the variables, which relates to the structure of the ET_0 equation. Any change in the structure of the equation causes a change in slope value. By improving the structure of the equation, the value of the slope will change; smaller values reduce the error in the ET_0 estimation. The second component that contributes to the error of ET_0 is the variables' uncertainty. This kind of uncertainty relates to the methods through which they are obtained. The methods presented by FAO to estimate the missing data can be improved. By improving the methods, it would be possible to estimate the missing variables with less uncertainty.

5.5. Summary

In this study, the error propagation approach was applied first for estimating the $RMSE$ of the ET_0 that was calculated with alternative data as recommended by FAO, and second for specifying the source of error in the ET_0 estimation. ΔET_0 was calculated via the error propagation approach. In the calculation procedure, the air temperature was considered the basic data, while the other three variables, R_s, e_a, and u_2, were treated as independent variables. From the results, it was confirmed that $RMSE$ is proportional to ΔET_0 with a proportionality coefficient close to unity and a regression coefficient of above 0.93 in three cases.

Furthermore, it was found that the error in the ET_0 estimation when calculated with alternative data was related to two sources: the variables' uncertainty that comes from the alternative data and the errors related to the combination of the variables in the equation i.e. the derivation of the function with respect to the variables, known as slope of the function.

Figure 5-1 Map of Japan with the study's locations numbered from 1 to 48.

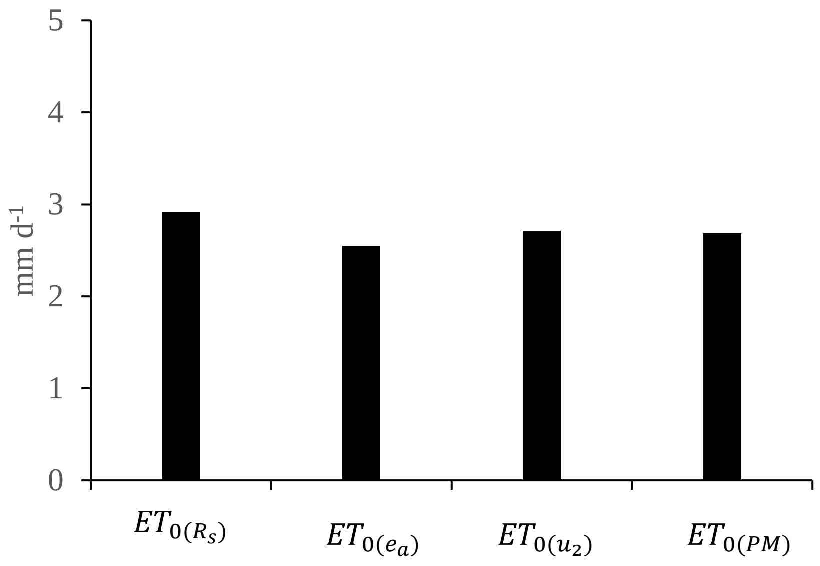

Figure 5-2 30 year average estimation of $ET_{0(st)}$ and ET_0 estimated with alternative data.

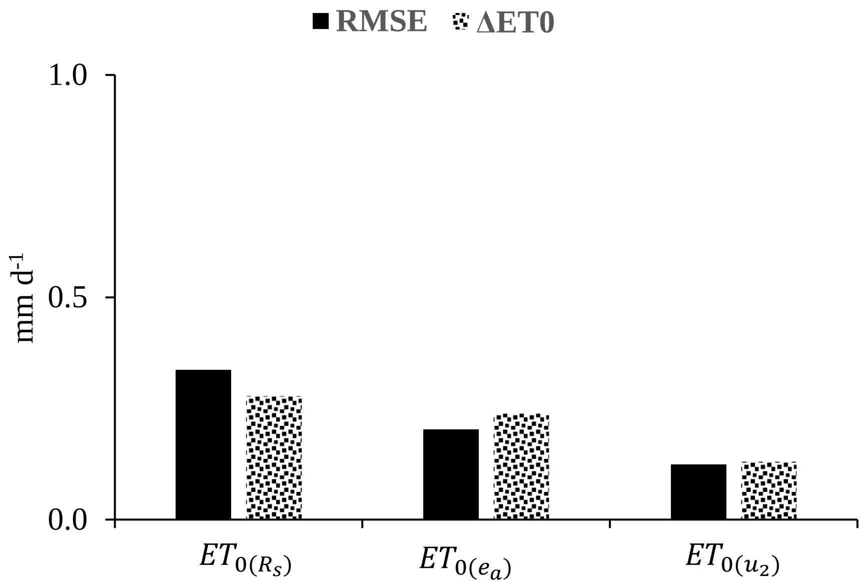

Figure 5-3 *RMSE* and ΔET_0 for ET_0 estimated with alternative data.

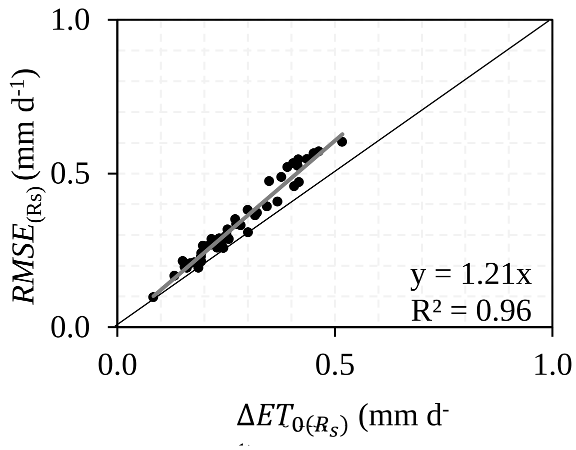

Figure 5-4 Relationship between $RMSE_{(R_s)}$ and $\Delta ET_{0(R_s)}$.

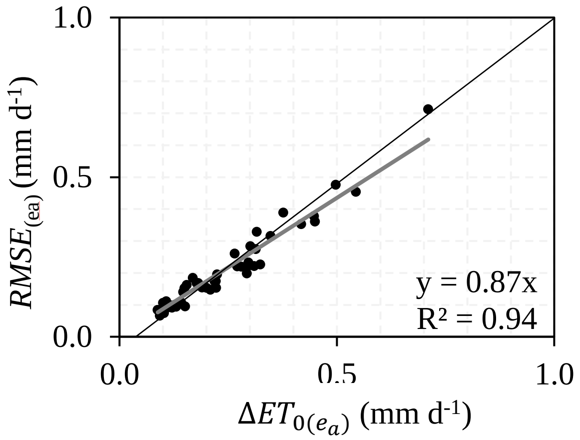

Figure 5-5 Relationship between $RMSE_{(e_a)}$ and $\Delta ET_{0(e_a)}$.

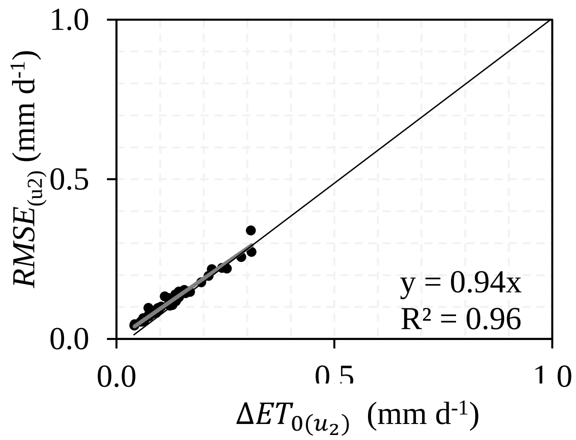

Figure 5-6 Relationship between $RMSE_{(u_2)}$ and $\Delta ET_{0(u_2)}$.

Table 5-1 Average record of the meteorological variables and estimated variables needed for calculating of the evapotranspiration

Station number	Station's location	Coordinate		Measured variables				Estimated variables	
		Elevation (m)	Latitude (Degree)	n (hour)	T_{Ave} (°C)	u_2 (m s^{-1})	RH (%)	R_s (MJ m^{-2} d^{-1})	e_a (kpa)
1	Wakkanai	3	45.41	4.0	7.1	3.0	75.3	11.1	0.29
2	Sapporo	17	43.06	4.7	9.4	1.8	68.8	12.2	0.33
3	Kushiro	5	42.98	5.3	6.6	2.5	76.8	12.3	0.28
4	Aomori	3	40.82	4.3	10.9	2.3	74.6	12.2	0.45
5	Akita	6	39.71	4.2	12.1	2.6	72.8	12.2	0.48
6	Morioka	155	39.69	4.6	10.8	2.0	73.7	12.4	0.42
7	Sendai	39	38.26	5.0	13.0	1.9	70.9	13.0	0.50
8	Yamagata	290	38.25	4.4	12.4	1.3	73.8	12.6	0.55
9	Niigata	0	37.89	4.5	14.3	2.4	71.3	12.9	0.58
10	Fukushima	67	37.75	4.8	13.7	1.5	68.8	12.9	0.53
11	Toyama	9	36.70	4.4	14.6	2.0	76.3	12.9	0.68
12	Kanazawa	6	36.58	4.6	15.1	2.2	71.0	13.2	0.67
13	Utsunomiya	119	36.54	5.3	14.6	1.7	69.4	13.5	0.55
14	Maebashi	112	36.40	5.9	15.3	2.0	62.3	14.2	0.51
15	Matsumoto	610	36.24	5.8	12.6	1.6	67.8	14.4	0.46
16	Kumagai	30	36.15	5.7	15.7	1.7	64.7	14.1	0.55
17	Fukui	9	36.05	4.5	15.1	1.8	74.8	13.1	0.70
18	Tokyo	20	35.69	5.3	16.7	2.0	61.8	13.7	0.56
19	Kofu	273	35.66	6.1	15.6	1.4	63.8	14.7	0.53
20	Chiba	3	35.06	5.3	16.4	2.4	67.9	13.8	0.60
21	Tottori	7	35.48	4.5	15.5	1.9	73.5	13.2	0.67
22	Matsue	17	35.45	4.6	15.5	2.2	75.5	13.3	0.69
23	Yokohama	39	35.43	5.5	16.5	2.4	66.7	14.1	0.58
24	Gifu	13	35.40	5.7	16.4	1.7	66.3	14.5	0.63
25	Hikone	87	35.27	5.0	15.2	1.9	73.8	13.8	0.66
26	Nagoya	51	35.16	5.8	16.5	2.1	65.8	14.6	0.60
27	Kyoto	36	35.01	4.8	16.5	1.3	65.6	13.4	0.63
28	Tsu	2	34.73	5.7	16.5	2.8	67.8	14.5	0.60
29	Kobe	3	34.69	5.5	17.0	2.4	65.8	14.4	0.59
30	Okayama	3	34.68	5.5	16.5	1.9	66.6	14.3	0.63
31	Osaka	1	34.68	5.5	17.4	1.9	63.4	14.4	0.62
32	Nara	90	34.67	4.9	15.5	1.0	72.5	13.7	0.62
33	Hiroshima	4	34.39	5.5	16.8	2.0	67.4	14.4	0.67
34	Takamatsu	34	34.31	5.6	16.8	1.8	67.1	14.5	0.66
35	Wakayama	14	34.22	5.7	17.1	2.2	65.5	14.7	0.64
36	Yamaguchi	5	34.16	5.1	16.1	1.3	72.5	14.0	0.72
37	Tokushima	2	34.06	5.7	17.0	2.2	66.8	14.7	0.63
38	Shizuoka	14	34.05	5.9	16.9	1.5	68.0	14.7	0.61
39	Matsuyama	41	33.84	5.5	16.9	1.4	66.8	14.5	0.69
40	Fukuoka	3	33.58	5.1	17.5	1.8	67.6	14.1	0.71
41	Kochi	1	33.56	5.9	17.5	1.3	68.5	14.9	0.69
42	Oita	5	33.23	5.4	16.9	1.8	69.0	14.5	0.70
43	Saga	3	33.07	5.4	17.1	2.4	69.9	14.4	0.73
44	Kumamoto	15	32.81	5.4	17.4	1.5	70.1	14.6	0.76
45	Nagasaki	7	32.73	5.1	17.6	1.6	70.3	14.2	0.77
46	Miyazaki	9	31.93	5.8	18.0	2.0	73.0	15.0	0.86
47	Kagoshima	4	31.55	5.3	19.0	1.9	69.8	14.6	0.86
48	Naha	51	26.21	4.7	23.5	3.2	73.1	14.6	1.62
	Average	48.6		5.2	15.4	1.9	69.5	13.8	0.6

n, measured sunshine hours; T_{Ave}, average air temperature; u_2, measured wind speed; RH measured relative humidity; R_s, solar radiation estimated with sunshine hours; e_a, actual vapor pressure estimated with relative humidity.

Table 5-2 Proportionality coefficient and the coefficient of determination between the correct reference evapotranspiration and those estimated with alternative data.

Station	$ET_{0(R_s)}$		$ET_{0(e_a)}$		$ET_{0(u_2)}$	
	k	R^2	k	R^2	k	R^2
1	1.01	0.98	0.93	0.93	0.96	0.98
2	1.09	0.97	1.06	0.98	0.97	0.98
3	1.09	0.98	0.93	0.99	0.99	0.99
:	:	:	:	:	:	:
:	:	:	:	:	:	:
46	1.06	0.96	0.99	0.99	0.99	0.99
47	1.04	0.97	0.93	0.96	0.99	0.94
48	0.94	0.88	0.83	0.87	0.92	0.96
Average	1.04	0.96	0.95	0.95	0.97	0.97

$ET_{0(R_s)}$, reference evapotranspiration estimated with alternative solar radiation data; $ET_{0(e_a)}$, reference evapotranspiration estimated with alternative, actual vapor pressure data; $ET_{0(u_2)}$, reference evapotranspiration estimated wit alternative wind speed data; k is proportional coefficient; R^2 is determination coefficient.

Table 5-3 Average values corresponding to the components of **Eq. 28**

	$\frac{\Delta ET_0}{\Delta x}$		Δx		ΔET_0	
R_s	3.02	$\frac{mm\ d^{-1}}{MJ\ m^2 d^{-1}}$	0.10	$MJ\ m^2 d^{-1}$	0.29	mm d^{-1}
e_a	0.16	$\frac{mm\ d^{-1}}{kPa}$	1.76	kPa	0.28	mm d^{-1}
u_2	0.55	$\frac{mm\ d^{-1}}{m\ s^{-1}}$	0.28	$m\ s^{-1}$	0.15	mm d^{-1}

$\frac{\Delta ET_0}{\Delta x}$, derivative of ET_0 with respect to the variables; Δx, variable's uncertainty; ΔET_0, error given by error propagation approach.

Chapter Six

Determining the Critical Distance Spatially for Sharing the Climatic Data Relating to Reference Evapotranspiration

6.1. Background

The validity of some alternative data in the ET_0 estimation was confirmed in variety of locations, however, some of the alternative data were not valid in some locations, depends upon the climatic regime of a place. Ganji and Kajisa (2018) reported that the ET_0 estimation yielded with relatively higher errors when alternative R_s and e_a were used in the calculation compared to the alternative u_2, in the case of humid climate of Japan. This may be the case for many locations over the globe.

To estimate ET_0 more accurate than that of using the FAO's alternative data there is a possibility to use the nearby station's measured data when the data of a given station is missing. However, the important matter is the determination of a critical distance (Xc) which is the upper limit of distance for data sharing between the stations. This is the distance inside of that range sharing data leads smaller error than that of using the FAO's alternative data as we are thinking. Xc might be different of the range Xh which can be determined by using different kind of models. One of the successful technique is using optimal approximation, which is applied in a geostatistical technique termed kriging (Warrick and Myers, 1987). Xh is the upper limit that longer that point data are no longer correlated. In this paper, from this approximation model equation and $\Delta ET_{0(Alt)}$, we attempted to determine the Xc spatially for sharing the data of R_s, u_2 and e_a when they are missing. The existence of Xc was not clear before analyzing.

In this paper, $\Delta ET_{0(st)}$ is the average errors between the two places produced from the actual measured data. $\Delta ET_{0(st)}$ is theoretically very small in a case if the distance between two places is zero, and it may increase for the increasing of the distance. While $\Delta ET_{0(Alt)}$ is the error produced using the alternative data those given by FAO's methodology in a given station. $\Delta ET_{0(Alt)}$ might be equal to $\Delta ET_{0(st)}$ at the Xc based on our prediction. At the distance larger than Xc, $\Delta ET_{0(st)}$ could become larger than $\Delta ET_{0(Alt)}$.

The typical concept proposed in this study is illustrated in Figure 6-1. In Figure 6-1, the X-axis shows the distance between the stations in (km), Y-axis shows $\Delta ET_{0(st)}$, $y(x)$ shows the model equation, Xh shows the proper range in which data are no longer correlated, and Xc shows the critical distance at which $\Delta ET_{0(Alt)}$ crosses the theoretical model equation's graph which is given by $\Delta ET_{0(st)}$.

6.2. Data and Analysis Method

The average meteorological data for a 30-year period used in this study were collected from the Japan metrological agency recorded in 48 places those are almost located in different prefectures over Japan, shown in **Figure 5-1** in Chapter 5. The numbers in **Figure 5-1** are in line with the numbers giving for each locations in **Table 5-1** in Chapter 5.

Structural analysis of $\Delta ET_{0(St)}$ estimates was initially used in order to identify the spatial variability features of $\Delta ET_{0(St)}$ over Japan. As of the first step, we began with getting $\Delta ET_{0(St)}$, computed with the values obtained from **Eq. 40** for all pairs of locations separated by distance. The right side of **Eq. 40** consists of two components, one is the variables' differentiation (Δz) produced from the average difference between the measured data of two stations, given as **Eq. 41** in which x is R_s, e_a or u_2. The second component is the slope of the functions obtained from the average values of station 1 and 2 given as **Eq. 42**. The value of the partial differential is the derivation of ET_0 with respect to the variables. The second step was fitting of model equation. According to the Delhomme (1978), the well-known models are the monomial, spherical, exponential and Gaussian. Here, the spherical model was experimentally selected (**Eq. 43**).

$$\Delta ET_{0(St)} = \Delta z \times \left(\frac{\Delta ET_0}{\Delta z_{1,2}}\right) \tag{40}$$

$$\Delta Z = \sqrt{\frac{1}{n}\sum_{i=1}^{n}(z_{1i} - z_{2i})^2} \tag{41}$$

$$\frac{\Delta ET_0}{\Delta z_{1,2}} = \frac{1}{2}\left(\sqrt{\frac{1}{m}\sum_{i=1}^{m}\left(\frac{\partial ET_0}{\partial z_1}\right)_i^2} + \sqrt{\frac{1}{m}\sum_{i=1}^{m}\left(\frac{\partial ET_0}{\partial z_2}\right)_i^2}\right) \tag{42}$$

$$y(x) = \begin{cases} c_0 + c\left(\frac{3h}{2a} - \frac{1}{2}\left(\frac{h}{a}\right)^3\right) & (0 < x \leq a) \\ c_0 + c & (a < x) \end{cases} \tag{43}$$

Where, $\Delta ET_{0(St)}$ is the average error between the two places produced from the actual measured data (mm d^{-1}), z_1 and z_2 are the measured values in the first and second locations, respectively, 1 and 2 are the suffixes of each place first and second, c_0 is nugget effect which we considered very small in this study, x is the distance between the two locations (km), a means range Xh in this paper, and $c_0 + c$ means sill.

To determine the Xc point, we computed $\Delta ET_{0(Alt)}$ using the error propagation approach. This approach was confirmed to approximate the root mean square error ($RMSE$) of ET_0 in Japan (Ganji and Kajisa, 2018). $\Delta ET_{0(Alt)}$ was calculated using **Eq. 44**. This consist of, the variable's differential ($\Delta z'$) yielded from the difference between measured data and alternative data at the same station (**Eq. 45**), and the partial differential of the function (**Eq. 46**). In **Eq. 40** and **44**, the FAO-56PM equation (**Eq. 47**) was transferred as **Eq. 48**. In this equation the components such as R_s, e_a and u_2 are independent, while c_1 to c_8 and e_s are constant. The variables such as R_s and e_a were calculated with measured climatic data, **Eqs. 3-4** in Chapter 1.

$$\Delta ET_{0(Alt)} = (\Delta z') \times \left(\frac{\Delta ET_0}{\Delta z'}\right) \tag{44}$$

$$\Delta z' = \sqrt{\frac{1}{n}\sum_{i=1}^{n}\left(z_i - z_{(Alt)i}\right)^2} \quad (45)$$

$$\frac{\Delta ET_0}{\Delta z'} = \sqrt{\frac{1}{m}\sum_{i=1}^{m}\left(\frac{\partial ET_0}{\partial z}\right)_i^2} \quad (46)$$

$$ET_0 = \frac{0.408\Delta(R_n - G) + \gamma \frac{900}{T_{Ave} + 273} u_2(e_s - e_a)}{\Delta + \gamma(1 + 0.34u_2)} \quad (47)$$

$$ET_0 = \frac{c_1R_s - (c_2 - c_3\sqrt{e_a})(c_4R_s - c_5) + c_6u_2(e_s - e_a)}{c_7 + c_8u_2} \quad (48)$$

where, $\Delta ET_{0(Alt)}$ is the error produced from the application of the alternative data in a given station (mm d^{-1}), $\Delta x'$ is the differentials between the measured data and alternative data in the same station, x and $x_{(Alt)}$ are the measured and alternative variables in a given station, R_n is the net radiation estimated with solar radiation data (MJ m^{-2} d^{-1}), G is the soil heat flux density (MJ m^{-2} d^{-1}), γ is the psychrometric constant (kPa ºC^{-1}), T_{Ave} is the daily average air temperature (ºC), u_2 is the daily average wind speed (m s^{-1}), e_s is the saturation vapor pressure (kPa), e_a is the actual vapor pressure (kPa), c_1 is given by $0.408\Delta(1-\alpha)$, c_2 is given by $0.34 \times 0.408\Delta\sigma(T_{max} + T_{min}) \div 2$, c_3 is given by $0.14 \times 0.408\Delta\sigma(T_{max} + T_{min}) \div 2$, c_4 is given by $1.35 \div R_{so}$, c_5 is equivalent to 0.35, c_6 is given by $900\gamma \div (T_{Ave} + 273)$, c_7 is given by $\Delta + \gamma$ in which Δ means the slope of the vapor pressure curve, c_8 is given by 0.34γ, α is the albedo (0.23), σ is the Stefan-Boltzmann constant, R_{so} is the clear-sky solar radiation (MJ m^{-2} d^{-1}), RH_{mean} is the mean relative humidity (%).

The FAO's alternative methodologies which were described in Chapter 3 (**Eq. 22** and **23**) are used in this chapter to estimate the alternative data for the missing of R_s, e_a and u_2.

6.3. Results

Figure 5-2 from **A** to **C** shows the approximated $y(x)$ curve, plots of $\Delta ET_{0(St)}$ versus the distance X, and $\Delta ET_{0(Alt)}$ as horizontal line. **Table 5-1** listed the values for Xh, Xc, X_{min}, X_{max}, $\Delta ET_{0(Alt)}$, c_0 and c. Xc was confirmed within the investigated distance in the case of R_s and e_a only, shown in **Figures 6-2A** to **B**. While no Xc exited within the investigated distance in the case of u_2, shown in **Figure 6-2C**.

6.4. Discussion

As we expected before the analysis that $Xc < Xh$, the results from the analysis met our expectation, however, Xh was found out of the investigated distance. The results of the analysis found two different cases corresponding to the **Figures 6-2A** to **C**.

A and B) $X_{min} < Xc < X_{max}$, this is the case corresponding to the R_s and e_a shown in **Figures 6-2A** and **B**, respectively. In the case, any X smaller than Xc will mean the range inside of which sharing data will be effective, while any X larger than Xc will not mean so. Because, the approximated $\Delta ET_{0(St)}$ on the line, i.e. $y(x)$ yielded below $\Delta ET_{0(Alt)}$ for $X < Xc$, while it was yielded above $\Delta ET_{0(Alt)}$ for $Xc < X$. This is implying that sharing the data among the stations within the rage of X smaller than Xc will be useful than that of using the FAO's alternative data of R_s and e_a.

C) $Xc < X_{min}$, this case was found out of our expectation. Xc was found very short and not critical. Therefore, applying the FAO's recommended methodology for alternative u_2 was found useful. On the other hand, the average measured u_2 yielded 1.9 ms^{-1} in the study area, given in **Table 5-1** which is almost close to the FAO's recommendation. In the case of missing u_2 we suggest to get the average u_2 in a given place if possible. Applying the average value should be very important which is free from the distance matter.

The fact that Xc very smaller than Xh means the alternative data recommended by FAO was much better than what we were thinking by seeing **Figure 6-1**.

6.5. Summary

Availability of the complete set of data is an extreme restriction to the application of the Penman-Monteith method in some places. Although, some producers have been recommended by FAO to estimate missing data using air temperature only, however, there is a possibility to use the nearby station's measured data when the data of a given station is missing. The important matter is the determination of a critical distance (Xc) for data sharing. In this paper, we attempted to determine the Xc spatially for sharing the data of R_s, u_2 and e_a when they are missing, by using the error propagation theory and experimental approximation equation. The existence of Xc was not clear before the analyzing. In a examined cases of Japan, the analysis leads to the following conclusions:

1) The existence of Xc was confirmed in the cases of R_s, e_a and u_2.
2) In our case, the Xc was in the range of the measured data for R_s and e_a. Therefore, the shared data can be recommended at a distance smaller than Xc, While the alternative data recommended by FAO can be selected at a distance larger than Xc. The Xcs were given as 2363 km and 341 km for R_s and e_a, respectively.

Xc was smaller than any X in case of u_2. Therefore, the alternative data recommended by FAO can be selected for all investigated distance. Xc was given as 20.11 km which was smaller than X_{min} which was 26.13 km.

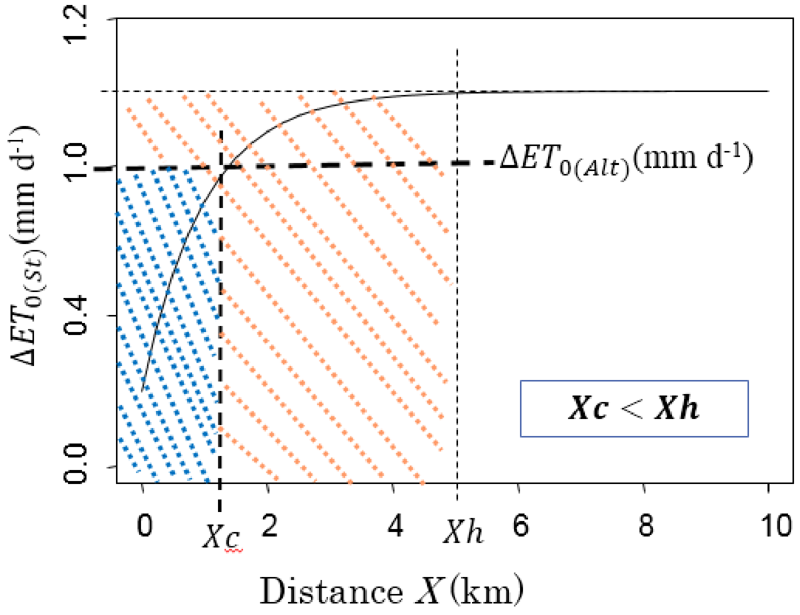

Figure 6-1 Model illustration depicts $\Delta ET_{0(St)}$, $\Delta ET_{0(Alt)}$, $y(x)$, Xc and the range Xh.

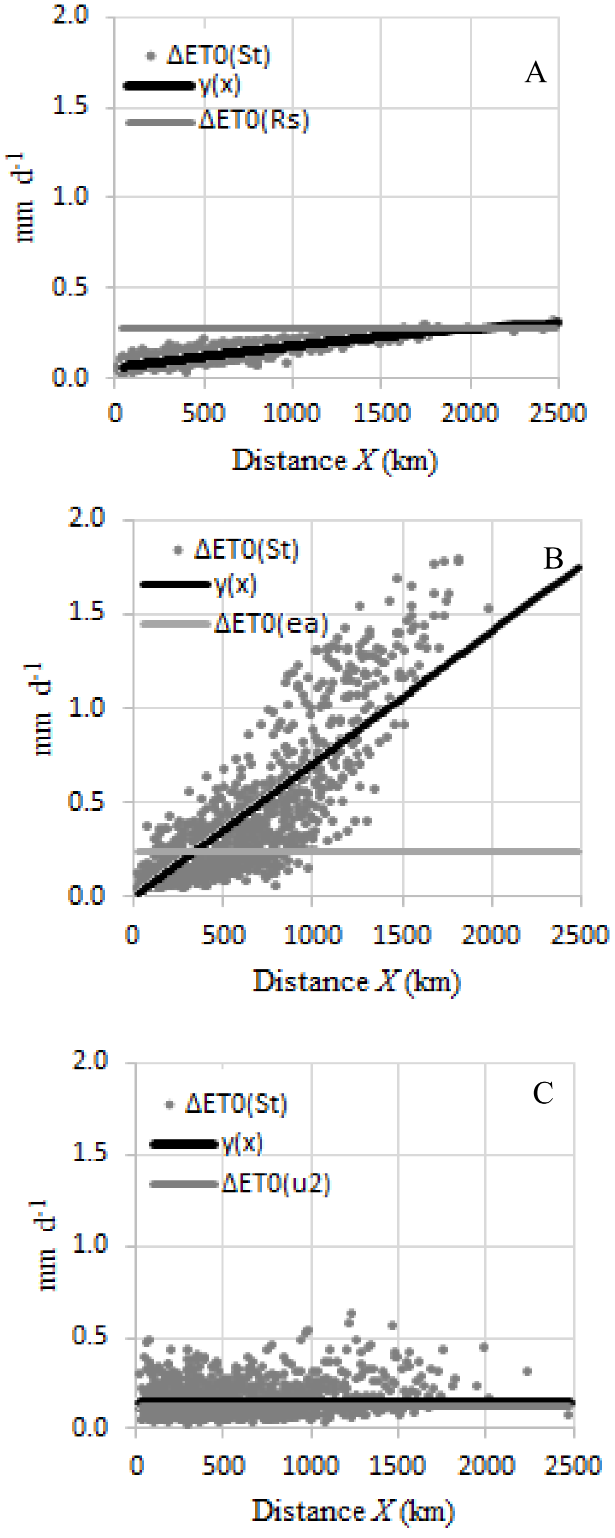

Figure 6-2 $\Delta ET_{0(St)}$, $\Delta ET_{0(Alt)}$ and the model $y(x)$; (A) is the case of R_s, (B) is the case of e_a, and (C) is the case of u_2.

Table 6-1 Details of different distances for the three cases

	Xc (km)	Xh (km)	X_{min} (km)	X_{max} (km)	c_0 (mm d^{-1})	c (mm d^{-1})	$\Delta ET_{0(Alt)}$ (mm d^{-1})
R_s	2,363.0	3,191.1	26.1	2,500.0	0.1	0.3	0.3
e_a	341.1	230,071.7	26.1	2,500.0	0.1	0.1	0.2
u_2	20.9	26.1	26.1	2,500.0	0.0	107.8	0.1

Chapter Seven

Conclusion

ET_0 is the main component of the irrigation water depth which is essential to estimate with high possible accuracy when calculating irrigation water depth. The accurate estimation of ET_0 depends upon several factors of which model selection can be one of the main factors. Many different models have been developed for calculating ET_0 based on their daily performances in a variety of conditions in the world. To select a best model for calculating ET_0 in a specific region, it is important to consider the accuracy offered by the selected model and the cost of data generation for the model. It is not easy to use the models that need high data demand in the regions facing with data scarcity. Therefore, either selecting models with less data requirement or alternative methods for obtaining missing data is essential in such a regions.

At the beginning, the author tried to estimate irrigation water depth using the FAO-56PM model in the West region of Afghanistan. The main problem with this model was its high data demand. There is only one metrological station in the West region that records the data, but it is not open for public application. Considering this limitation, the author attempted to examine the other well-known models which require fewer data. Six well-known models plus the FAO-56PM were compared against ET_{pan} under the climate condition of the West region of Afghanistan. Results showed that, all examined models produced estimates that were significantly different from ET_{pan} in the windy period, with the exception of the ET_{0PM} model. This model showed the closest agreement with ET_{pan}, except in the high rate. The rate of ET_0 reaches above 10 mm d^{-1} in the period from June to September, which is high enough and has a lot of unexpectedness. One of the important phenomenon in this period in the West region of Afghanistan is the extreme climate condition, means high air temperature, low humidity, and especially strong persistent wind speed. The author conducted the second experiment with the aim to assess the FAO-56PM throughout the course of the year under the climate condition of the West region. The results confirmed that, the high rate of ET_0 related to the extreme climate condition, dominates during the period from June to September. While the rest of the year, the climate condition was normal as well as the rate of ET_0 was moderate. The root mean square error ($RMSE$) reached above 1 mm d^{-1} during the windy period. On the other hand, the wind speed was found highly correlated to the $RMSE$. It could be confirmed that this kind of error becomes larger when ET_0 becomes larger than 10 mm d^{-1}.

Although, the FAO-56PM model was confirmed the best model under the climate condition of the West region of Afghanistan, however, application of this model is limited due to data scarcity. To overcome this problem, alternative data of solar radiation, humidity, and wind speed can be obtained from the procedures adopted in the FAO paper no. 56. In this study, the validity of the alternative data was assessed with respect to the climate conditions in three different regions in Afghanistan. The results confirmed that, the alternative data of wind speed and humidity were not highly valid under the windy conditions for estimating ET_0. While the alternate solar radiation was valid because the estimation of ET_0 was not affected when alternative solar radiation used in the calculation.

When the alternative wind speed and humidity data were found erroneous in the ET_0 calculation, to overcome this probable, the idea of sharing data from the nearby metrological station was proposed. However, the important matter was the determination of an effective distance (Xc) for data sharing. In this study, it was attempted to determine the Xc spatially for sharing the missing data. By using the error propagation theory and experimental approximation equation in a examined cases of Japan, the existence of Xc was confirmed in the cases of solar radiation and actual vapor pressure. Therefore, sharing the data of solar radiation and actual vapor pressure can be recommended at a distance smaller than Xc, while the alternative data recommended by FAO can be selected at a distance larger than Xc. in the case of wind speed Xc was found smaller than any X in the investigated distance.

In any region, to confirm the validly of FAO-56PM model when estimating with alternative data, $RMSE$ is essential to be calculated. To calculate $RMSE$, ET_0 should be estimated with both complete and alternative data. In the other hand, $RMSE$ dose not specify the source of error in a model equation. In this study, the error propagation approach was proposed to estimate $RMSE$ and to quantify the source of error in the FAO-56PM equation. From the results, it was found that $RMSE$ is highly proportional to ΔET_0 and it can be estimated within 10% error by using the theoretical equation of error propagation. As well as, it was found that the source of error in the model equation is not only the alternative data, but the combination of the variables (equation structure) is the source of error as well.

References

Allen, R. G., Jensen, M. E., Wright, J. L. and Burman, R. D.: "Operational estimates of reference evapotranspiration," J. Agronomy, vol. 81(4), 1989, pp. 650-662.

Allen R. G. and Pruitt W. O. : "FAO-24 reference evapotranspiration factors," J. of irrigation and drainage engineering, vol. 117(5), 1991, pp. 758-773.

Allen, R. G., Pereira-Luis, S., Dirk, R. and Martin, S. : "FAO Irrigation and drainage paper no. 56," Food and Agriculture Organization of the United Nations, vol. 56, 1998, pp. 97-156.

Alkaeed C., Flores K., Jinno K., & Tsutsumi A., "Comparison of several reference evapotranspiration methods for Itoshima Peninsula area, Fukuoka, Japan," Kyushu University, vol. 66(1), Mar. 2006.

Alexandris S, Kerkides P, Liakatas A. : "Daily reference evapotranspiration estimates by the ''Copais'' approach,".J. Agricul. Water Manage. vol. 82, 2005, pp. 371–386.

Brutsaert W., & Parlange M. B., "Hydrologic cycle explains the evaporation paradox," J. of Nature, vol. 396(30), 1998, pp. 30-30.

Bandyopadhyay A., Bhadra A., Raghuwanshi N. S., & Singh R. : "Temporal trends in estimates of reference evapotranspiration over India," Int. Journal of Hydrologic Engineering, vol. 14(5), 2009,pp. 508-515.

Conceição M. A. F., "Reference evapotranspiration based on class A-pan evaporation," Scientia Agricola, vol. 59(3), 2002, pp. 417-420.

Chen D., Ge Gao, Chong-Yu Xu, Jun Guo, & Ren G. : "Comparison of the Thornthwaite method and pan data with the standard Penman-Monteith estimates of reference evapotranspiration in China," Climate Research, vol. 28(2), 2005, pp. 123-132.

Chiew F. H. S., Kamaladasa N. N., Malano H. M., & McMahon T. A. : “Penman-Monteith, FAO-24 reference crop evapotranspiration and class-A pan data in Australia,” Agricultural Water Management, vol. 28(1), 1995, pp. 9-21.

Cuenca R. H., “Irrigation system design: An engineering approach,” Prentice-Hall, Englewood Cliffs, vol. 552, 1989.

Cordova, M., Galo, C. R., Patricio, C., Bradford, W. and Rolando, C. : “Evaluation of the Penman-Monteith (FAO-56 PM) method for calculating reference evapotranspiration using supplementary data application to the wet Páramo of Ecuador,” J. Mountain Research and Development, vol. 35 (3), 2015, pp. 230-39.

Droogers, P. and Allen R. G. : “Estimating reference evapotranspiration under inaccurate data conditions,” J. Irrigation and Drainage Systems, Vol. 16 (1), 2002, pp33-45.

Doorenbos J. : “Guidelines for predicting crop water requirements,” FAO Irrigation and Drainage Paper 24, 1997, pp. 15-29.

Frevert D. K., Hill R.W., & Braaten B.C. : “Estimation of FAO evapotranspiration coefficients,”. Journal of Irrigation and Drainage Engineering, vol. 109(2), 1983, pp. 265-270.

Ganji H., Rahmany A. S., Kajisa T, Kondo M., & Narioka H. : “Comparison of the crop water need between actual wind condition and zero wind simulation; wind velocity within 24-hour interval in Herat, Afghanistan,” 20th Int. Conf. on ISSAAS, Tokyo University of Agriculture, 2014, pp. 91.

Ganji, H., Kajisa, T. : "Applying the error propagation approach for predicting root mean square error of the reference evapotranspiration when estimated with alternative data," J. Agri. Eng. (under review).

Ganji H., Rahmany A., Narioka H., Kondo T., & kajisa T. : "Effect of the 120-day winds on Agriculture and environmental condition in Herat, Afghanistan," 4th Int. Conf. on Geotechnique, Construction Materials and Environment, Brisbane Australia, 2014.

Ganji H., Kajisa T., Kondo M., & Rostami B. : "Re-Examining the validity of reference evapotranspiration in Herat Afghanistan," Int. Journal of GEOMATE, vol. 12(30), 2017, pp. 61-66.

Gundekar H. G., Khodke U. M., Sarkar S. : "Evaluation of pan coefficient for reference crop evapotranspiration for semi-arid region," Irrig Sci. vol. 26, 2008, pp. 169–175.

Gavilan P., Lorite I. J., Tornero S., & Berengena J. : "Regional calibration of Hargreaves equation for estimating reference ET in a semiarid environment," Agricultural Water Management, vol. 81, 2005, pp. 257–281.

Grismer M. E., Orang M., & Matyac S. : "Pan evaporation to evapotranspiration conversion methods," J. Irrig. Drain. Eng., vol. 128(3), 2002, pp. 180-184.

Garcia, M., Raes, D., Allen, R. G. and Herbas, C., "Dynamics of reference evapotranspiration in the Bolivian highlands (Altiplano)," J. Agricultural and forest meteorology, vol.125(1-2), 2004, pp. 67-82.

Gocic, M. and Trajkovic, S. : "Software for estimating reference evapotranspiration using supplementary data," J. computers and electronics in agriculture, vol.71(2), 2010, pp. 158-162.

Gerard B. M. H. : "Error propagation in environmental modeling with GIS," CRC press, 1998.

Gavilán P., Lorite, I. J., Tornero S., Berengena J., "Regional calibration of Hargreaves equation for estimating reference evapotranspiration in a semiarid environment," J. Agricult. Water Manage., vol. 81, 2006, pp. 257-281.

Hanson R. L., "Evapotranspiration and droughts," National Water Summary, 1988, pp. 99-104.

Haith D. A, & Leslie L. S. : “Generalized watershed loading functions for stream flow nutrients,” J. of JAWRA, vol. 23(3), Jun. 1987, pp. 471-478.

Hargreaves G. H., & Allen R. G. : “History and evaluation of Hargreaves evapotranspiration equation,” J. of Irrigation and Drainage Engineering, vol. 129(1), Feb. 2003, pp. 53-63.

Hargreaves, G. H. and Samani, Z. A. : “Reference crop evapotranspiration from temperature,” J. Applied engineering in agriculture, vol.1(2), 1985, pp.96-99.

Irmak S., Irmak R., Allen R. G., & Jones W. J. : “Solar and net radiation-based equations to estimate reference evapotranspiration in humid climates,” J. of irrigation and drainage engineering, vol. 129(5), Oct. 2003, pp. 336-347.

Irmak S., Haman D. Z., & Jones J.W. : “Evaluation of class-A pan coefficients for estimating reference evapotranspiration in humid location,” J. of Irrigation and Drainage Engineering, vol. 128(3), 2002, pp. 53-159.

Jabloun, M. D., and Sahli, A. : "Evaluation of FAO-56 methodology for estimating reference evapotranspiration using limited climatic data: Application to Tunisia," J. Agricul. Water Manage., vol. 95, 2008, pp. 707-715.

Kimbal, J. S., Running, S. W. and Nemani, R. : “An improved method for estimating surface humidity from daily minimum temperature,” J. Agricultural and Forest Meteorology, vol. 85(1–2), 1997, pp.87-98.

Mudelsee, M. : “Estimating Pearson's correlation coefficient with bootstrap confidence interval from serially dependent time series,” J. of Mathematical Geology, vol. 35(6), 2003, pp. 651-665.

Oudin L., Frederic H., Michel C., Perrin C., Andreassian V., Anctil F., & Loumagne C. : “Which potential evapotranspiration input for a lumped rainfall–runoff model? Part 2—towards a simple and efficient potential evapotranspiration model for rainfall–runoff modelling,” Hydrology, vol.303, 2005, pp. 290–306.

Orang M. : “Potential accuracy of the popular non-linear regression equations for estimating pan coefficient values in the original and FAO-24 tables,” Unpublished Rep., Calif. Dept. of Water Resources, Sacramento, 1998.

Popova, Z., Milena, K. and Luis, S. P. : “Validation of the FAO methodology for computing ET0 with supplementary data, Application to South Bulgaria,” J. Irrigation and Drainage, vol.55(2), 2006, pp. 201-215.

Pereira A.R, Pruitt W.O. : "Adaptation of the Thornthwaite scheme for estimating daily reference evapotranspiration," J. Agricul. Water Manage., vol. 66, 2004, pp. 251–257.

Qureshi A.,& Sarwar A., “Water resources management in Afghanistan-the issues and options,” IWMI, vol. 49. 2002.

Sabziparvar A. A., Tabari H., Aeini A., & Ghafouri M. : “Evaluation of class A pan coefficient models for estimation of reference crop evapotranspiration in cold semi-arid and warm arid climates,” Water resources management, vol. 24(5), 2010, pp. 909-920.

Steduto P., Caliandro A., Rubino P., & Mechlia N. B. : “Penman-Monteith reference evapotranspiration estimates in the Mediterranean region,” Proceedings of int. conf. on evapotranspiration and irrigation scheduling, 1996, pp. 357-364.

Sentelhas P. C., & Folegatti M. V. : “Class A pan coefficients to estimate daily reference evapotranspiration,” Revista Brasileira de Eng. Agre. Ambiental, vol. 7(1), 2003, pp. 111-115.

Sentelhas, P. C., Terry, J. G. and Eduardo, A. S. : “Evaluation of FAO Penman-Monteith and alternative methods for estimating reference evapotranspiration with missing data in southern Ontario, Canada,” J. Agricultural Water Management, vol. 97(5), 2010, pp. 635-44.

Singh P. K., Patel S. K., Jayswal P., & Chinchorkar S. S. : "Usefulness of class A Pan coefficient models for computation of reference evapotranspiration for a semi-arid region," MAUSAM, vol. 65(4), 2014, pp. 521-528.

Snyder R. L. : "Equation for evaporation pan to evapotranspiration conversions," J. Irrig. Drain. Eng., vol. 118(6), 1992, pp. 977-980.

Temesgen B., Simon E., Baryohay D., & Kent F. : "Comparison of some reference evapotranspiration equations for California," Irrigation and Drainage Engineering, vol. 131(1), 2005.

Warrick, A.W., and Myers, D. E. : "Optimization of sampling locations for variogram calculations," J. Wat. Res. Res, vol. 23, 1987, pp. 496- 500.

Xu C. Y., & Singh V. P. : "Evaluation and generalization of radiation-based methods for calculating evaporation," Hydrological Processes, vol. 14, 2000, pp. 339-349.

Appendix

To compute **Eqs. 1-5** in Chapter 1, the following equations are needed.

$$P = 101.3\left(\frac{293-0.0065Z}{293}\right)^{5.26} \quad (49)$$

$$\gamma = 0.665 \times 10^{3}P \quad (50)$$

$$\Delta = \frac{4098\left[0.6108exp\left(\frac{17.27T_{ave}}{T_{ave}+273.3}\right)\right]}{(T_{ave}+273.3)^{2}} \quad (51)$$

$$R_{a} = \frac{24(60)}{\pi}0.0820d_{r}[\omega_{s} + \cos(\varphi)\cos(\delta)\sin(\omega_{s})] \quad (52)$$

$$d_{r} = 1 + 0.033\cos\left(\frac{2\pi}{365}J\right) \quad (53)$$

$$\delta = 0.409sin\left(\frac{2\pi}{365}J - 1.39\right) \quad (54)$$

$$\omega_{s} = arccos[-\tan(\varphi)\tan(\delta)] \quad (55)$$

$$N = \frac{24}{\pi}\omega_{s} \quad (56)$$

$$Rso = (0.25 + 0.50)Ra \quad (57)$$

Where P is the Atmospheric pressure (kPa), Z is the elevation above sea level (m), γ is the psychrometric constant (kPa °C^{-1}), Δ is the slope of saturation vapor pressure curve at air temperature (kPa °C^{-1}), R_a is the extraterrestrial radiation (MJ m^{-2} d^{-1}), φ is the latitude (rad), d_r is the inverse relative distance Earth-Sun, δ is the solar decimation (rad), J is the number of the day in the year between 1 (1 January) and 365 or 366 (31 December), ω_s is the sunset hour angle (rad), N is the daylight hours, Rso clear-sky solar radiation (MJ m^{-2} d^{-1}).